https://doi.org/10.1093/plcell/koac038 THE PLANT CELL 2022: 34: 2019–2037

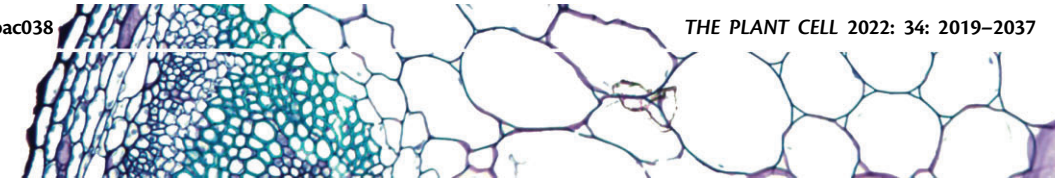

Research Article

Non-autonomous stomatal control by pavement cell turgor via the K^+ channel subunit *AtKC1*

Manuel Nieves-Cordones [1,*,†,‡] Farrukh Azeem [1,†] Yuchen Long [2,†] Martin Boeglin [1] Geoffrey Duby [1] Karine Mouline [1] Eric Hosy [1,†] Alain Vavasseur [3] Isabelle Chérel [1] Thierry Simonneau [4] Frédéric Gaymard [1] Jeffrey Leung [5] Isabelle Gaillard [1] Jean-Baptiste Thibaud [1,6] Anne-Aliénor Véry [1,*,‡] Arezki Boudaoud [2,†] and Hervé Sentenac [1,*]

1 Biochimie et Physiologie Moléculaire des Plantes, UMR BPMP, Univ Montpellier, CNRS, INRAE, Montpellier SupAgro, Montpellier 34060, France
2 Laboratoire Reproduction et Développement des Plantes, Univ Lyon, ENS de Lyon, UCB Lyon 1, CNRS, INRA, F-69342 Lyon, France
3 CEA Cadarache DSV DEVM LEMS UMR 163, CNRS/CEA, F-13108 St Paul Lez Durance, France
4 INRA Laboratoire d'Ecophysiologie des Plantes sous Stress Environnementaux, Place Viala, 2, F-34060 Montpellier Cedex 1, France
5 Université Paris-Saclay, INRAE, AgroParisTech, CNRS, Institut Jean-Pierre Bourgin (IJPB), 78000 Versailles, France
6 Institut des biomolécules Max Mousseron (UMR 5247 CNRS-UM-ENSCM) Campus CNRS, 1919 route de Mende, F-34293 Montpellier Cedex 05, France

*Author for correspondence: herve.sentenac@inrae.fr (H.S.), mncordones@cebas.csic.es (M.N.-C.), anne-alienor.very@cnrs.fr (A.-A.V.)
†Present addresses
Manuel Nieves-Cordones, Departamento de Nutrición Vegetal, CEBAS-CSIC, Campus de Espinardo, 30100 Murcia, Spain.
Yuchen Long, Department of Biological Sciences, National University of Singapore, Singapore 117558, Singapore.
Farrukh Azeem, Department of Bioinformatics and Biotechnology, Govt. College University, Faisalabad, Pakistan.
Eric Hosy, Interdisciplinary Institute for Neuroscience, University of Bordeaux, F-33077 Bordeaux Cedex, France.
Arezki Boudaoud, LadHyX, CNRS, Ecole polytechnique, Institut Polytechnique de Paris, 91120 Palaiseau, France.
‡Senior authors
M.N.-C. carried out the mutant phenotyping, cell-specific complementation experiments, and MP recordings by microelectrode impalement. F.A. performed the gene expression and guard cell complementation analyses. G.D. carried out the mutant phenotyping experiments and the epidermal plasmolysis assays. K.M., A.V., T.S., and F.G. identified the mutant phenotype and conducted the first transpiration analyses. M.B., E.H., and A.-A.V. carried out the patch-clamp analyses on guard cell and pavement cell protoplasts. M.N.-C., A.V., and I.G. performed the stomatal aperture measurements. I.C., J.L., and T.S. contributed to the project conception. I.G. supervised the gene expression, mutant phenotyping, and complementation experiments. Y.L. performed the AFM measurements. Y.L. and A.B. designed the AFM experiments and analyzed the AFM data. H.S. and J.-B.T. jointly supervised the whole project. M.N.-C., H.S., J.-B.T., J.L., and A.-A.V. wrote the manuscript.
The author(s) responsible for the distribution of materials integral to the findings presented in this article in accordance with the policy described in the Instructions for Authors (https://academic.oup.com/plcell) are: Manuel Nieves-Cordones (mncordones@cebas.csic.es) and Anne-Aliénor Véry (anne-alienor.very@cnrs.fr).

Abstract

Stomata optimize land plants' photosynthetic requirements and limit water vapor loss. So far, all of the molecular and electrical components identified as regulating stomatal aperture are produced, and operate, directly within the guard cells. However, a completely autonomous function of guard cells is inconsistent with anatomical and biophysical observations hinting at mechanical contributions of epidermal origins. Here, potassium (K^+) assays, membrane potential measurements, microindentation, and plasmolysis experiments provide evidence that disruption of the *Arabidopsis thaliana* K^+ channel subunit gene *AtKC1* reduces pavement cell turgor, due to decreased K^+ accumulation, without affecting guard cell turgor. This results in an impaired back pressure of pavement cells onto guard cells, leading to larger stomatal apertures. Poorly

Received February 22, 2021. Accepted January 28, 2022. Advance access publication February 14, 2022

IN A NUTSHELL

Background: The water that plants absorb from the soil is mainly lost through evaporation at the leaf surface across microscopic pores called stomata. On the other hand, these pores also allow the diffusion of CO_2 from the atmosphere to the internal tissues for photosynthesis. Stomata are surrounded by two specialized cells, called guard cells. Changes in guard cell turgor allow them to swell or shrink for enlarging or narrowing the pore. This control is aimed at preventing excessive water loss. Gaining knowledge on the underlying mechanisms will provide tools to optimize water use by plants.

Question: The epidermal cells surrounding the guard cells, called pavement cells, form an anatomical obstacle that limits the movement of the guard cells. Their turgidity exerts a counter-pressure on the guard cells that opposes stomatal opening. The molecular mechanisms underlying this non-autonomous control of stomatal aperture by guard cells are poorly understood.

Findings: We show that disruption of the *Arabidopsis thaliana* K^+ channel subunit gene *AtKC1* reduces pavement cell turgor, due to decreased K^+ accumulation, without affecting guard cell turgor. This results in a decrease in the back-pressure of pavement cells onto guard cells. The *atkc1* mutation increases the sensitivity of the pavement cell membrane electrical potential to external K^+, revealing an impaired control of K^+ transport properties. Restoration of the wild-type stomatal phenotype requires expression of *AtKC1* in the pavement cells but also in another epidermal cell type, the trichomes. Thus, the whole epidermis appears to contribute to the non-autonomous control of transpirational water loss.

Next steps: The family of K^+ channels to which AtKC1 belongs is strongly conserved in plants and comprises AtKC1 homologs in every species. Whether the present information is translatable to crops should be investigated. The role of trichomes in regulating stomatal aperture via AtKC1 also deserves further research.

rectifying membrane conductances to K^+ were consistently observed in pavement cells. This plasmalemma property is likely to play an essential role in K^+ shuttling within the epidermis. Functional complementation reveals that restoration of the wild-type stomatal functioning requires the expression of the transgenic *AtKC1* at least in the pavement cells and trichomes. Altogether, the data suggest that *AtKC1* activity contributes to the building of the back pressure that pavement cells exert onto guard cells by tuning K^+ distribution throughout the leaf epidermis.

Introduction

In land plants, the epidermis is covered by a non-permeable waxy cuticle, and the diffusion of CO_2 from the atmosphere to inner photosynthetic tissues takes place through microscopic pores present on the leaf surface. Each of these pores is surrounded by a pair of osmocontractile cells, named guard cells, together forming a stoma. The physical continuum provided by the stomata between the leaf inner tissue and the atmosphere also enables transpiration, which has however to be tightly controlled to avoid desiccation.

The epidermis comprises three main types of clonally related cells: pavement cells, guard cells, and trichomes. Embedded within the epidermal cell layer, guard cells can be in direct contact with surrounding pavement cells (e.g. in *A. thaliana*; Supplemental Figure S1, left photo column), or associated with subsidiary cells (Nguyen et al., 2017) to form a stomatal complex (Gray et al., 2020). The molecular and osmotic machinery responsible for the changes in guard cell turgor that either open (Tominaga et al., 2001; Jammes et al., 2014) or close the stomatal pore has been deeply investigated (Jezek and Blatt, 2017). All components regulating stomatal movements, even the cell-to-cell mobile abscisic acid (ABA) stress hormone (Bauer et al., 2013), are produced and act directly within the guard cells. For instance, in response to low atmospheric or soil humidity, ABA initiates stomatal closing by binding to a subfamily of cytosolic receptors within the guard cells to activate a phosphorylation-based signaling cascade leading to reduced cell turgor by modulating interdependent H^+, potassium (K^+), and anion fluxes (Hedrich, 2012; Jezek and Blatt, 2017). In angiosperms, mature guard cells are thought to lack plasmodesmata with adjoining cells (Wille and Lucas, 1984; Palevitz and Hepler, 1985), reinforcing the notion of their self-sufficient functioning. Highly purified guard cell protoplasts have been extensively used to characterize in detail the ABA-induced events that include changes in ion transport activities (Jezek and Blatt, 2017) as well as transcriptomic (Leonhardt et al., 2004; Wang et al., 2011), proteomic (Zhao et al., 2008), and metabolomic profiles (Jin et al., 2013; Misra et al., 2015; Zhu and Assmann, 2017).

K^+ is a major osmoticum in this machinery (Humble and Raschke, 1971; Talbott and Zeiger, 1996; Hedrich, 2012; Jezek

and Blatt, 2017; Britto et al., 2021). K^+ fluxes into, or out of, guard cells, resulting in stomatal opening or closure, respectively, involve voltage-gated K^+ channels of the Shaker family (Blatt, 2000; Véry and Sentenac, 2003; Pandey et al., 2007; Kim et al., 2010; Hedrich, 2012; Véry et al., 2014). Gene expression studies, electrophysiological analyses, and reverse genetics approaches carried out in Arabidopsis have revealed that K^+ influx into guard cells, leading to stomatal opening, is strongly dependent on expression of the inwardly rectifying hyperpolarization-activated Shaker K^+ channels *KAT1* and *KAT2* (K^+ channel in *A. thaliana* 1 and 2) (Lebaudy et al., 2008, 2010), while the efflux of K^+ from guard cells, allowing stomatal closure, involves expression of the outwardly rectifying depolarization-activated Shaker K^+ channel *GORK* (Hosy et al., 2003).

The large body of cellular and molecular information leads to the conclusion that guard cells possess all necessary molecular and electrical components in stomatal control. This understanding is, however, unmoored from the biophysical and anatomical approaches of stomatal regulation within its epidermal context, in which the embedded guard cells are subjected to mechanical and physiological exertions from their neighboring pavement/subsidiary cells (Jezek et al., 2019). For example, stomatal conductances can show considerable microheterogeneity in the leaf even when this organ is kept in a constant environment. This has been attributed to variable or unstable hydraulic interactions between guard cells with their surrounding pavement cells, usually within leaf sectors defined anatomically by vein patterns (Mott and Buckley, 2000). Also, at the cell level, when a series of reductions of turgor are experimentally imposed on both guard and pavement cells of epidermal strips, by increasing the concentration of an osmotically active solute in the external solution, the stomatal aperture does not narrow, as would be expected if guard cells responded independently of pavement cells. Rather, the pore aperture will widen in a first phase. When the concentration of the external solute is further increased, the stomatal aperture will then narrow in a more gradual second phase. In contrast, if the turgor of the pavement/subsidiary cell is selectively ablated, the stomatal aperture will simply narrow in a "monotonic" way with the increase in external solute concentration (MacRobbie, 1980). These observations suggest that, within an epidermal layer, the stomatal aperture is not autonomously regulated, but conjointly set by, at least, the relative turgor that opposes the guard cells with the surrounding pavement cells. Much is still unknown about the mechanisms that underlie the non-autonomous stomatal response, such as the molecular, cellular, and physiological bases of the interacting mechanisms, and the responsible epidermal cell types or their locations in the leaf. Here, we show that the Shaker channel gene *AtKC1* (*A. thaliana* K^+ channel 1) (accession number AT4G32650) contributes to these mechanisms.

Shaker channels, which dominate the plasma membrane conductance to K^+ in most cell types, are encoded by a family of nine members in Arabidopsis (Véry et al., 2014). These channels are sensitive to voltage and activated by either membrane depolarization for K^+ efflux (outwardly rectifying channels), or membrane hyperpolarization allowing K^+ influx (inwardly rectifying channels). They are tetrameric proteins, and the four subunits that assemble to form a functional protein can be encoded by the same Shaker gene (giving rise to a homotetrameric channel) or different Shaker genes (heterotetrameric channel) (Daram et al., 1997; Urbach et al., 2000; Jegla et al., 2018). The Shaker subunit encoded by *AtKC1* (At4G32650) has been termed a "silent" Shaker channel subunit (Reintanz et al., 2002) because it does not form functional channels on its own but only when in complex with other inwardly rectifying channel subunits to modulate the functional properties of the channel, including voltage sensitivity (Duby et al., 2008; Geiger et al., 2009; Honsbein et al., 2009; Jeanguenin et al., 2011; Zhang et al., 2015; Wang et al., 2016).

AtKC1 is expressed in roots and leaves (Reintanz et al., 2002; Pilot et al., 2003). In the root, it is expressed in the periphery cells, where it associates with the *AKT1* inward Shaker subunit and thereby plays a role in channel-dependent K^+ uptake from the soil (Geiger et al., 2009; Honsbein et al., 2009). In leaves, *AtKC1* is expressed in the whole epidermal tissue, that is in trichomes, hydathodes, pavement cells, and guard cells (Pilot et al., 2003; Supplemental Figure S1), in contrast to the two other well-studied inward Shaker channel genes *KAT1* and *KAT2* whose expression pattern in the leaf epidermis is restricted to guard cells (Nakamura et al., 1995; Pilot et al., 2001). In this report, we show that *AtKC1* contributes to stomatal aperture regulation by modulating conflicting turgors of guard cells and surrounding pavement cells.

Results

Disruption of *AtKC1* impairs the control of stomatal aperture

The role of *AtKC1* in the leaf epidermis was investigated using a loss-of-function Arabidopsis line, *atkc1–2*, obtained in the Wassilewskija (Ws) ecotype (Jeanguenin et al., 2011). Leaves excised from *atkc1–2* plants were found to lose more water than leaves excised from wild-type (WT) plants (Figure 1A). Furthermore, stomatal conductance measured in intact leaves (Figure 1B) and transpiration rates in whole-plant assays during both light and dark periods (Figure 1C) were larger in *atkc1–2* than in WT plants. In agreement with these observations, in vitro measurements of stomatal aperture on leaf epidermal strips yielded larger values in *atkc1–2* than in WT plants, regardless of dark or light conditions (stimuli of stomatal closure and opening, respectively) (Figure 1D). Stomatal density was not affected by the *atkc1–2* mutation (Supplemental Figure S2). Transformation of the *atkc1–2* mutant with a construct-allowing expression of *AtKC1* under the control of its own promoter region led to a WT phenotype in each of these experiments (Figure 1, A–D), providing evidence that the stomatal defects of the

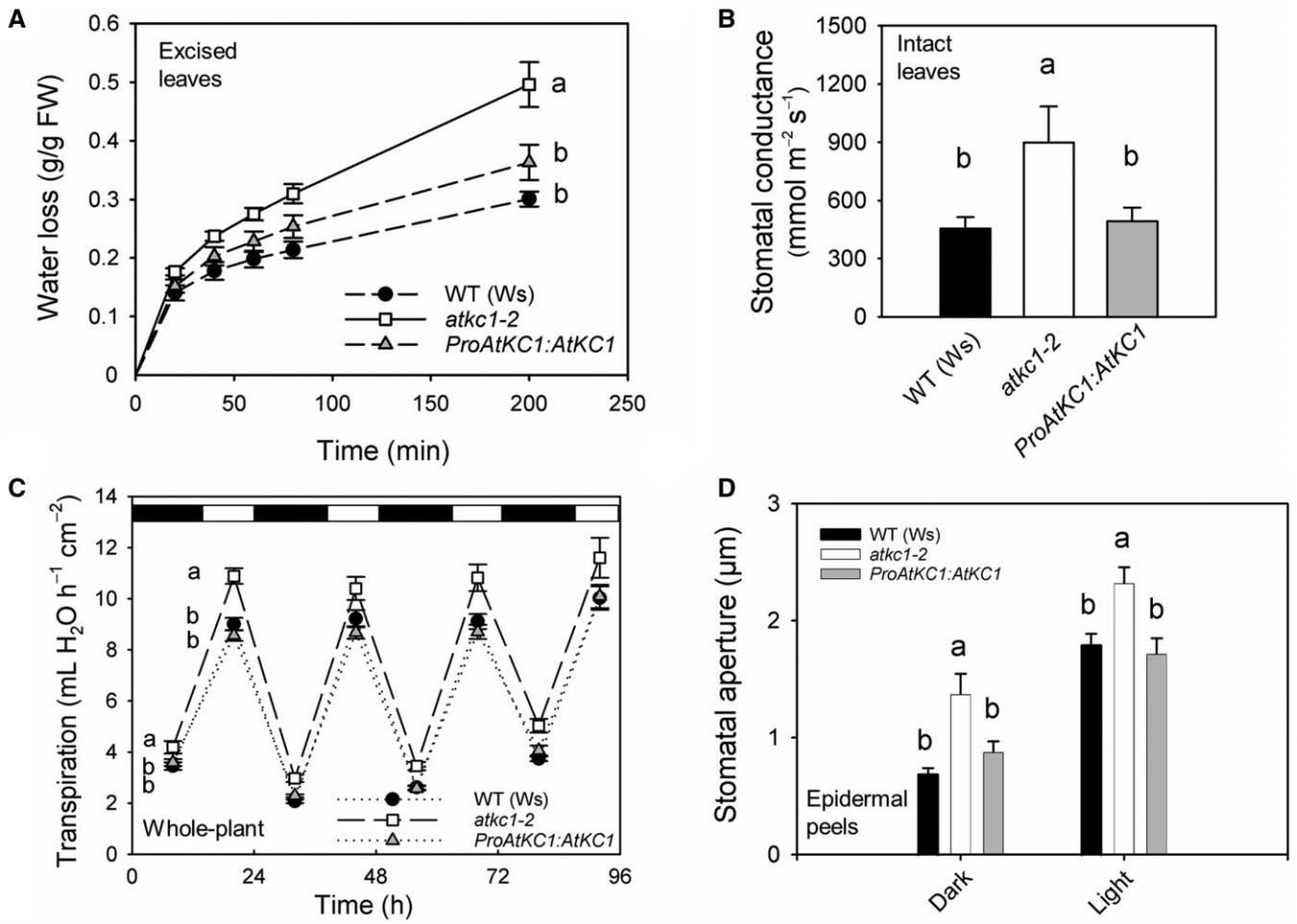

Figure 1 Impaired control of stomatal aperture and transpirational water loss in *atkc1–2*-mutant plants. A, Transpirational water loss from excised leaves. The second leaf was excised from WT (Ws ecotype), *atkc1–2*, and *ProAtKC1:AtKC1*-complemented *atkc1–2* plants. Excised leaf water loss was deduced from the decrease in leaf weight. B, Leaf water conductance measured on intact leaves with a porometer. C, Transpiration rates in whole-plant assays. D, Stomatal aperture in WT, *atkc1–2*, and *ProAtKC1:AtKC1*-complemented *atkc1–2* plants. Before stomatal aperture measurements, epidermal strips were kept in the dark for 2 h (dark treatment) or in dark for 2 h, followed by 2 h in the light (light treatment) in a 40 mM K^+ solution. A–D, Means ± SE. In (A)–(C), n = 5, 9, and 11, respectively; in (D), n = 6 values, each value corresponding to ∼100 stomata. Letters depict significant group values after ANOVA and Tukey's post hoc test. In C, for the statistical analysis, the data obtained during the four consecutive days were pooled, taking into account the corresponding day cycle.

atkc1–2 mutant plants resulted from the absence of *AtKC1* functional expression.

Patch-clamp analyses of the membrane conductance to K^+ in epidermal cells

The patch-clamp technique was used to investigate the membrane conductance to K^+ in protoplasts enzymatically obtained from WT and *atkc1–2* epidermal strips. The electrophysiological recordings carried out in WT guard cell protoplasts yielded a classical current–voltage (*I–V*) curve, displaying the typical strong rectification of both the inward and outward K^+ currents (Figure 2) in agreement with literature data (Schroeder et al., 1987; Hosy et al., 2003; Lebaudy et al., 2008). This rectification results from the fact that the K^+ channels mediating K^+ transport across the guard cell membrane are either activated by membrane hyperpolarization and dedicated to K^+ influx, or activated by membrane depolarization and then dedicated to K^+ efflux. Within a large range of voltages, from about −150 to 0 mV in the experiment described in Figure 2, the two populations of channels are inactive and the membrane is almost impermeable to K^+. Such channels are said to be "rectifiers": they mediate a K^+ current in only one direction, either into or out from the cell. Very similar *I–V* curves were obtained in the WT and in the *atkc1–2* mutant (Figure 2), which led to the conclusion that the absence of *AtKC1* expression had no significant impact on the membrane conductance to K^+ in guard cells.

No patch-clamp analysis of pavement cell protoplasts has been reported in Arabidopsis to our knowledge. Protoplasts from pavement cells were obtained by shorter enzymatic cell-wall digestion compared with guard cell protoplasts. Pavement cell protoplasts could be distinguished from guard cell protoplasts based on their larger size and from

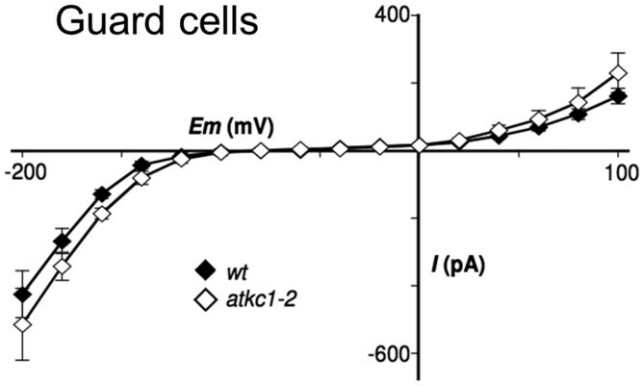

Figure 2 Shaker-like K^+ channel activity in guard cells from WT and *atkc1–2*-mutant plants (Ws ecotype). Guard cell protoplast current/voltage relationships. Means ± SE; n = 8 and 10 for the WT and mutant genotypes, respectively. External K-glutamate concentration was 100 mM.

contaminating mesophyll protoplasts (if any in the preparation) based on the absence of chloroplasts.

Different types of current traces could be distinguished in the WT pavement cell protoplasts (Figure 3 and Supplemental Figure S3, A–C). The recorded traces/protoplasts were operationally sorted into two major categories, according to the presence (Figure 3) or absence (see below, Supplemental Figure S3, A–C) of an inward current component displaying a time-dependent activation, reminiscent of a Shaker-type slowly activating conductance (Véry and Sentenac, 2002).

The membrane conductance to K^+ of WT protoplasts displaying the Shaker-type slowly activating currents was analyzed in more detail. The *I–V* curve obtained for this type of protoplast in the presence of 105 mM K^+ in the external solution (Figure 3, B and E, black symbols) crosses the *x*-axis close to the K^+ equilibrium potential, estimated to be close to −7 mV (the K^+ concentration of the pipette solution and external bath being close to 140 and 105 mM, respectively), as expected since K^+ was the single permeable ion present at a high concentration in these solutions. A major result is that these *I-V* curves reveal a rather low level of rectification (Figure 3, B and E), when compared with that displayed by the guard cell *I–V* curve (Figure 2). Adding 10 mM Ba^{2+} (a classical K^+ channel blocker: Schroeder et al., 1987; Wegner et al., 1994; Roelfsema and Prins, 1997; Pilot et al., 2001; Su et al., 2005; Rohaim et al., 2020) resulted in a strong inhibition of the recorded currents (Figure 3, A–C), the magnitude of the inhibition appearing to be slightly voltage-dependent (Figure 3C). Decreasing the external concentration of K^+ from 105 to 15 mM shifted the current reversal potential by about −40 mV (Figure 3, D and E; theoretical shift by ca. −49 mV expected for a membrane permeable to K^+ only). Altogether, these results indicated that the currents were mainly channel mediated and carried by K^+ ions.

Patch-clamp recordings were carried out in parallel experiments (alternating measurements on WT and mutant plants grown simultaneously) to compare the electrical properties of pavement cell protoplasts from WT and *atkc1–2* plants. Among 28 protoplasts from WT pavement cells, 10 (ca. 36%) belonged to the first category, that is displaying a Shaker-type time-dependent activation of inward currents (as shown in Figure 3F). In agreement with the data shown by Figure 3, B and E, the *I–V* curve obtained from these 10 protoplasts displays a low level of rectification (Figure 3H, black symbols). In the second category of protoplasts, that is characterized by the absence of an inward current component displaying a time-dependent activation (18 protoplasts out of the 28 ones), at least three patterns of current traces could be identified (Supplemental Figure S3, A–C). The *I–V* curves corresponding to these recordings also displayed a rather weak level of rectification (lower panels in Supplemental Figure S3, A–C), when compared with that observed in guard cell protoplasts (Figure 2). The current recordings obtained in the *atkc1–2* mutant protoplasts could be sorted into the same categories as those defined for the WT protoplasts, according to the presence or absence of a detectable time-dependent inward Shaker-type component. From 32 protoplasts, 8 (25%) displayed such a component (Figure 3G), which was also characterized by a low level of rectification (Figure 3H, open symbols), and 24 protoplasts belonged to the other category (Supplemental Figure S3, D–F). No significant impairment of the membrane conductance to K^+ was detected in the *atkc1–2* protoplasts classified as belonging to the former category, that is displaying the Shaker-type component, when compared with the corresponding WT protoplasts (Figure 3H). In the other category, each of the different types of current patterns that were recorded in the *atkc1–2* pavement cell protoplasts seemed to have a counterpart among the current patterns observed in the corresponding WT protoplasts (Supplemental Figure S3). This whole set of data did not provide evidence that the *atkc1–2* mutation affected the membrane conductance to K^+ in every pavement cell.

Loss of *AtKC1* expression in guard cells does not underlie the *atkc1–2* mutant stomatal phenotype

AtKC1 transcripts were found to be at higher levels, by about five times, in whole leaf extracts than in guard cells (Figure 4A, right panel). Furthermore, *AtKC1* transcripts in guard cell protoplasts were at lower levels than those of *KAT1* and *KAT2* (Figure 4A, left panel), the major contributors to the Shaker inward conductance in guard cells (Lebaudy et al., 2008, 2010; Hedrich, 2012).

In the epidermis, the *KAT1* promoter (*ProKAT1*) is specifically active in guard cells (Nakamura et al., 1995). A *ProKAT1:AtKC1* construct introduced into *atkc1–2* mutant plants did not rescue the stomatal phenotype of *atkc1–2* in the dark, in the light, and after a treatment with the stress hormone ABA, well known to induce stomatal closure (Figure 4B). Detection of *AtKC1* transcripts in leaves of *atkc1–2*-mutant plants transformed with this *ProKAT1:AtKC1* construct (Supplemental Figure S4A)

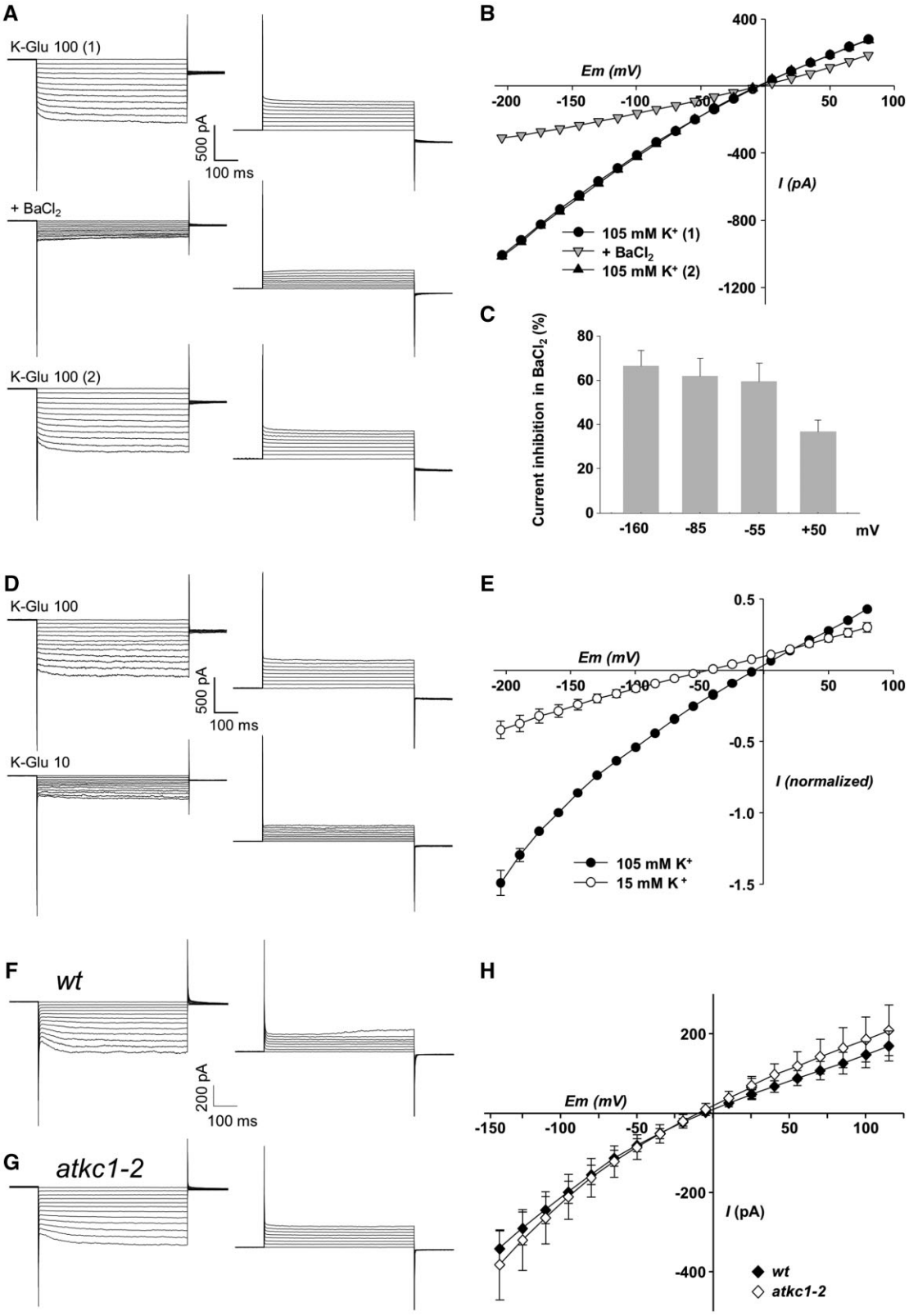

Figure 3 Weakly inwardly-rectifying K^+ channel activity in pavement cells from WT and *atkc1–2*-mutant plants (Ws ecotype). A–C, Typical weakly inwardly rectifying K^+ currents recorded in pavement cell protoplasts and their blockage by 10 mM external $BaCl_2$. A, Example of inward and outward current traces (right and left panels, respectively), recorded in the presence of 100 mM K-glutamate (total K^+ concentration: 105 mM) and successively before $BaCl_2$ addition (top panels), in the presence of $BaCl_2$ (middle panel), and after $BaCl_2$ rinse (lower panels). B, Corresponding current/voltage relationships. C, Current inhibition in the presence of $BaCl_2$ at negative and positive voltages. Means ± SE; n = 7. D and E, Effect of change in external K-glutamate concentration on the weakly inwardly rectifying currents in pavement cell protoplasts. D, Example

provided first evidence that the absence of complementation was not due to expression issues. A crucial objective was then to check whether the *ProKAT1* promoter was actually active and allowed expression of AtKC1 subunits in guard cells of the *atkc1–2* mutant in the experimental conditions that had previously allowed the defect in stomatal aperture control to be observed in the *atkc1–2* mutant (Figure 1). In planta, we did not succeed in detecting the fluorescence of *AtKC1-GFP* translational fusions expressed under the control of the *ProKAT1* promoter (or under control of any of the promoters described below when stably expressed in Arabidopsis transgenic plants). So far, to our knowledge, translational *AtKC1-GFP* fluorescence in plant cells has only been observed with strong constitutive promoters such as that from the gene of an H^+-ATPase (Duby et al., 2008; Jeanguenin et al., 2011; Nieves-Cordones et al., 2014) or 35S (Honsbein et al., 2009). We thus developed an alternative strategy by taking advantage of the fact that *AtKC1* can associate with the guard cells *KAT1* and *KAT2* inward Shaker channel subunits and thereby form heteromeric channels (Jeanguenin et al., 2011) to develop a dominant negative approach as described by Lebaudy et al. (2008). A dominant-negative form of *AtKC1*, *AtKC1–DN*, was substituted for *AtKC1* in the previous *ProKAT1:AtKC1* construct. *AtKC1–DN* encodes a mutated channel subunit (obtained by site-directed mutagenesis) in which large and positive residues (R) are present in the pore region (Jeanguenin et al., 2011). These residues plug the channel permeation pathway when *AtKC1-DN* subunits associate with other inwardly rectifying Shaker subunits, including *KAT1* and *KAT2* (Jeanguenin et al., 2011). After introduction into the *atkc1–2* mutant, the new construct, *ProKAT1:AtKC1–DN*, was found to reduce stomatal aperture (Supplemental Figure S4B), providing evidence that *AtKC1–DN* was expressed in *atkc1–2*-mutant guard cells, inhibiting inward channel activity, and thus that *ProKAT1* was actually active in *atkc1–2* guard cells under our experimental conditions. Altogether, these results provided the first indication that the absence of *AtKC1* expression in guard cells alone could not be considered as the main cause of the *atkc1–2*-mutant stomatal phenotype.

Disruption of *AtKC1* results in decreased K^+ accumulation in leaf epidermis and reduced turgor pressure in pavement cells

K^+ contents were measured in whole leaves, in leaf margins (isolated 2-mm-width strips) enriched with hydathodes and in epidermal strips. Compared with the WT, the overall K^+ status of *atkc1–2* was not substantially altered in whole leaves (Figure 5), in agreement with previous analyses (Jeanguenin et al., 2011), nor was it altered in leaf margins (Figure 5). In contrast, K^+ contents in epidermal strips were significantly lower, by 42 mM, in the mutant than in WT plants, when compared on a fresh weight basis (from Figure 5, the FW/DW ratio being 9.3 ± 0.3, $n = 12$). Such a difference in K^+ content between *atkc1–2* and WT plants could hardly be ascribed to guard cells alone but rather to pavement cells, because of the relatively lower abundance and volume of guard cells in the leaf epidermis (see Supplemental Figure S1).

The hypothesis that reduced K^+ contents in *atkc1–2* pavement cells would decrease the turgor of these cells was then checked via three independent experimental approaches. First, recent improvements in atomic force microscopy (AFM) allowed us to quantify turgor pressure in living plant cells (Beauzamy et al., 2015). Data obtained under similar conditions as those used for in vitro measurements of stomatal aperture in epidermal strips (under light and in the presence of stomatal aperture solution; Figures 1D and 4B) showed that the pavement cell turgor pressure was weaker (by ~0.15 MPa) in *atkc1–2* than in WT plants (Figure 6A, left panel). In contrast, measurements performed in parallel on the same leaves in the same experimental conditions did not reveal any significant difference in guard cell turgor between the WT and *atkc1–2* plants (Figure 6A, right panel), providing further support to the hypothesis that *AtKC1* plays a role in regulating stomatal aperture from another cell type than guard cells. During these measurements, we have also noted that within the same WT leaf, the turgor pressure was higher, on average by about two times, in the guard cells than in the pavement cells (Figure 6A; note the difference in *y*-axis scale between the left and right panels).

In a second series of experiments, we assessed the effects of increasing the concentration of mannitol in the solution bathing epidermal strips on pavement cell plasmolysis. Relative to the WT, 40–60 mM less mannitol was needed to plasmolyze 50% of *atkc1–2* pavement cells (Figure 6B), which indicated reduced osmotically active solute contents in *atkc1–2* pavement cells.

The third series of experiments was inspired by classical analyses of the effects of external medium osmolarity on stomatal aperture. MacRobbie (1980) showed that stomatal aperture in epidermal strips responded differently to increasing the external osmolarity depending on whether the surrounding pavement cells were dead (killed by acid treatment) or alive (see "Introduction"). We investigated the

Figure 3: (continued)
of inward and outward current traces (right and left panels, respectively) recorded successively in 100 mM K-glutamate (top panels) and 10 mM K-glutamate (lower panels; total K^+ concentration: 15 mM). E, Current/voltage relationships in the two external K-glutamate conditions. Currents were normalized in each protoplast by the current value obtained in 100 mM K-glutamate at −160 mV. Means ± SE; $n = 7$. F and G, Representative inward and outward (right and left panels, respectively) Shaker-like K^+ current traces in WT (F) and *atkc1–2* (G) pavement cell protoplasts. H, Pavement cell protoplast Shaker-like current/voltage relationship in WT and *atkc1–2*-mutant plants. External K-glutamate concentration: 100 mM. Means ± SE; $n = 8$ for both the WT and the mutant genotypes. The concentration of K^+ (essentially as glutamate salt) in the pipette solution and in the bath solution was 140 and 105 mM, respectively, which results in a K^+ equilibrium potential of close to −7 mV.

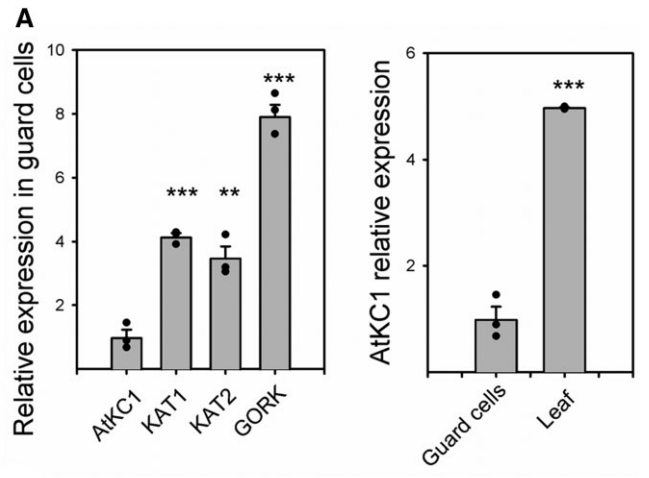

Figure 4 The defect in stomatal aperture displayed by the *atkc1–2* mutant does not result from loss of *AtKC1* expression in guard cells. A, Relative expression of *AtKC1* compared with that of other Shaker channels in guard cells (left panel) and relative expression of *AtKC1* in guard cells compared with that in leaves (right panel). Expression levels determined by RT-qPCR experiments. B, Stomatal aperture in WT plants, in *atkc1–2*-mutant plants, and in *atkc1–2*-mutant plants transformed with either the complementing *ProAtKC1:AtKC1* construct (see Figure 1) or with a construct, *ProKAT1:AtKC1*, rendering *AtKC1* expression dependent on the activity of the promoter of *KAT1*, a Shaker channel gene whose expression in guard cells is specific of this cell type in leaf epidermis (see also Supplemental Figure S4). "Dark" and "light" treatments: stomatal aperture was measured under dark or light as described in Figure 1D. "Light + ABA" treatment: 10 µM ABA was applied for 2 h to light-treated strips before stomatal aperture measurement. A and B, Means ± SE. For (A), $n = 3$ pools of 5–6 plants, and ** and *** denote $P < 0.01$ and < 0.001 in a two-tailed Student's *t* test (comparison *AtKC1* expression to that of *KAT1*, *KAT2*, or *GORK*, left panel, and *AtKC1* expression in guard cells versus *AtKC1* expression in leaves, right panel). For (B), $n = 6–10$ values, each value corresponding to ~60 stomata. Letters depict significant group values after ANOVA and Tukey's post hoc test.

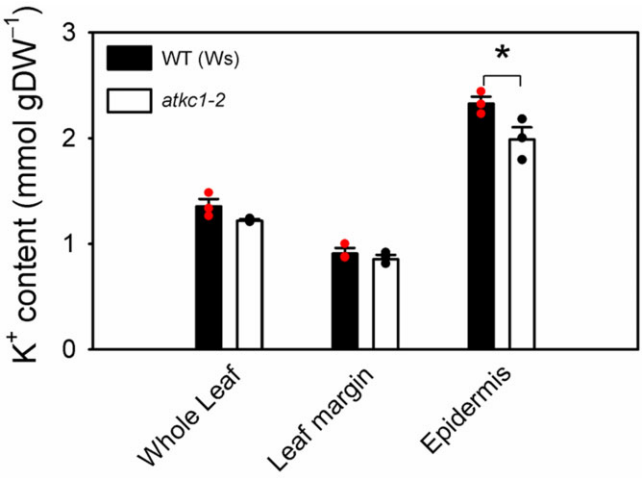

Figure 5 Disruption of *AtKC1* leads to reduced K^+ contents in leaf epidermis. K^+ contents in whole leaf, leaf margin, and leaf epidermis in WT and *atkc1–2*-mutant plants. Means ± SE; $n = 3$ pools, each one obtained from nine leaves (*$P < 0.05$, using two-tailed Student's *t* test).

relationship between stomatal aperture and external medium osmolarity, this time independently of the alive/dead status of the pavement cells, but rather in the presence or absence of *AtKC1* expression. Stomatal aperture was measured in epidermal strips bathed in standard medium (as in Figure 1D experiment) supplemented with mannitol at increasing concentrations in order to raise the external osmolarity. In *atkc1–2* epidermal strips, the stomatal aperture decreased monotonically (Figure 6C). Conversely, in WT epidermal strips, the stomatal aperture displayed a slight increase in a first step and then decreased when the mannitol concentration was further increased (Figure 6C). Such a non-monotonic relationship between extracellular osmotic potential and stomatal aperture is reminiscent of the results of MacRobbie (1980) discussed above. It can be classically explained as follows. Increasing the external osmolarity decreases the turgor of both the guard cells and the pavement cells by the same amount. The resulting turgor reduction in pavement cells tends to increase the stomatal aperture; while in guard cells, it tends to reduce this aperture. The balance of these opposite effects determines the final stomatal aperture at a given external osmolarity. Thus, the relation between stomatal aperture and the external osmolarity can be non-monotonic. Reciprocally, such a non-monotonic response provides evidence that guard cell turgor is not the only determinant of stomatal aperture and that the turgor of the surrounding pavement cells exerts a back pressure onto guard cells, thereby playing a role in the control of stomatal aperture. The results displayed in Figure 6C therefore indicate that a back pressure was exerted on guard cells by surrounding pavement cells in WT epidermal strips, but that this phenomenon did not occur in *atkc1–2* epidermal strips.

Altogether, these three series of experiments indicated that reduced K^+ contents decreased the turgor in *atkc1–2* pavement cells and thereby the back pressure that these cells can exert onto guard cells. They thus provided evidence that *AtKC1* contributes to control of stomatal aperture from the surrounding pavement cells.

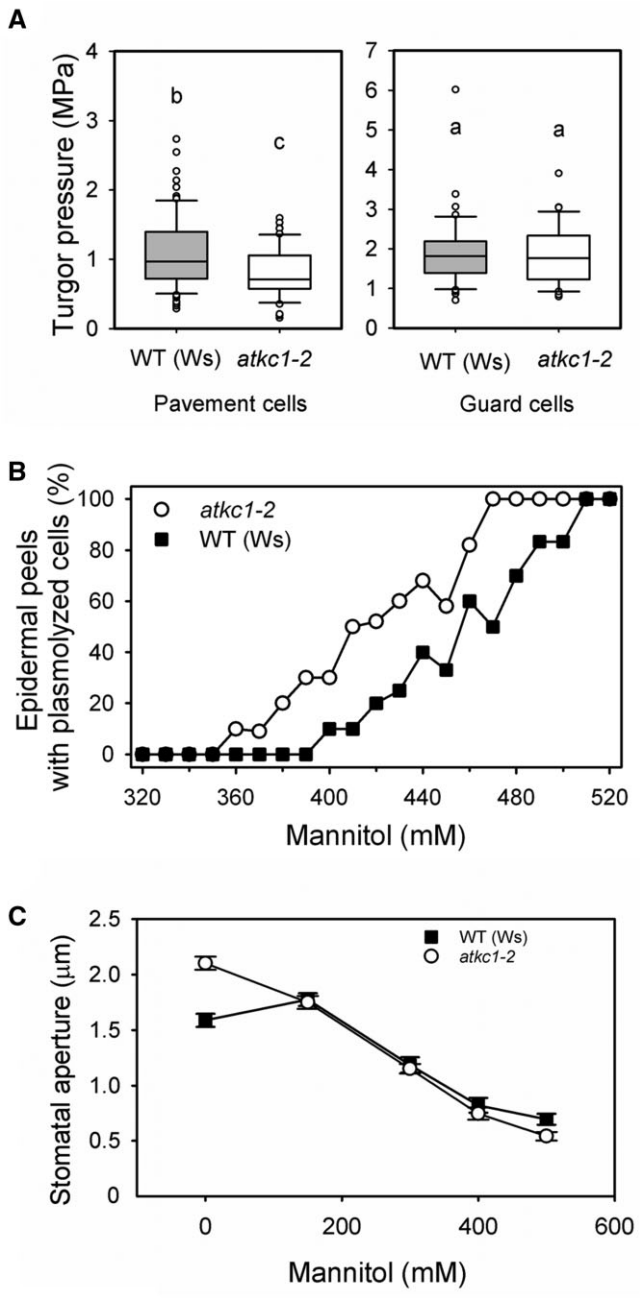

Figure 6 Disruption of *AtKC1* leads to reduced turgor pressure in pavement cells but not in guard cells. A, Boxplots depicting turgor pressure values obtained with AFM in WT and *atkc1*–2 pavement cells (left panel) and guard cells (right panel). Upper and lower whiskers: 1.5 times the IQR (first to third interquartile range); border of the boxes: first and third quartile; central line: median. Letters depict different group values after Student's *t* test ($P < 0.05$). For guard cells, $n = 46$ for the WT genotype and 32 for the *atkc1*–2-mutant genotype. For pavement cells, $n = 86$ for the WT and 51 for the mutant genotype. B, Disruption of *AtKC1* results in decreased osmotic pressures in leaf epidermis as deduced from plasmolysis curves obtained by measuring the percentage of epidermal strips displaying plasmolyzed cells when bathed for 5 min in the presence of mannitol. Ten–twelve strips were examined for each genotype and mannitol concentration. C, Effect on stomatal aperture of adding mannitol to the solution bathing epidermal strips from WT or *atkc1*–2-mutant plants. $n = 92–120$ from six leaves for each mannitol concentration and genotype.

Membrane potential measurements in pavement cells

Electrical consequences of the *atkc1*–2 mutation in pavement cells were looked for in planta by recording the resting membrane potentials (MPs) successively at two different external K^+ concentrations, 0.1 and 10 mM, using the microelectrode impalement technique. Significantly less negative MP values were recorded in *atkc1*–2-mutant plants, when compared with WT control plants, by ca. 20 and 48 mV at 0.1 mM and 10 mM K^+, respectively (Figure 7A). The observation of less-negative MPs in pavement cells of the mutant plants is consistent with the lower K^+ content of the epidermis displayed by these plants, when compared with the WT control plants (Figures 5 and 6B). In such experiments, the magnitude of the membrane depolarization induced by an increase in external K^+ is classically interpreted as reflecting the relative K^+ permeability of the membrane (Spalding et al., 1999). The depolarization induced in pavement cells by the increase in K^+ concentration from 0.1 to 10 mM was significantly smaller in the WT than in *atkc1*–2 pavement cells (Figure 7B–D), revealing a higher relative K^+ permeability in the *atkc1*–2-mutant cells, which is consistent with the role of *AtKC1* as a negative regulator of Shaker inward K^+ channels (Jeanguenin et al. 2011; see "Discussion").

Expression of *AtKC1* in several epidermal cell types is required to complement the *atkc1*–2-mutant stomatal phenotype

AtKC1 was expressed in *atkc1*–2-mutant plants using different promoters with overlapping epidermal cell-specificity to determine further cell types, besides pavement cells, in which *AtKC1* would affect stomatal aperture control: *ProCER5* (*At1G51500*) (Pighin et al., 2004), *ProOCT3* (*At1G16390*) (Kufner and Koch, 2008), *ProGL2* (*At1G79840*) (Szymanski et al., 1998), promoter of the *Uncharacterized Protein Kinase* gene *At1G66460* (Jakoby et al., 2008), *ProFMO1* (*At1G19250*) (Olszak et al., 2006), *ProCYP96A4* (*At5G52320*), and *ProKCS19* (*At5G04530*). The expression patterns of these promoters were experimentally confirmed in transgenic Arabidopsis by fusing them to the glucuronidase (*GUS*) reporter gene. These observed patterns (Supplemental Figure S1 and Table 1; see description below) were entirely consistent with the eFP Browser data (Supplemental Table S1).

Each of these seven promoters was used to direct transgenic expression of *AtKC1* in the *atkc1*–2-mutant tissues. The capacity of the transgenes to complement the mutant phenotype was checked in a first series of experiments by measuring stomatal aperture in the transformed plants (T3 homozygous transgenic lines) in light conditions as previously performed for the complementing construct *ProAtKC1:AtKC1* and the non-complementing one *ProKAT1:AtKC1* (Figure 4B).

Five of the seven constructs were found not to complement the mutant stomatal phenotype (Figure 8A and Table 1). These were *ProKCS19:AtKC1*, *ProOCT3:AtKC1*,

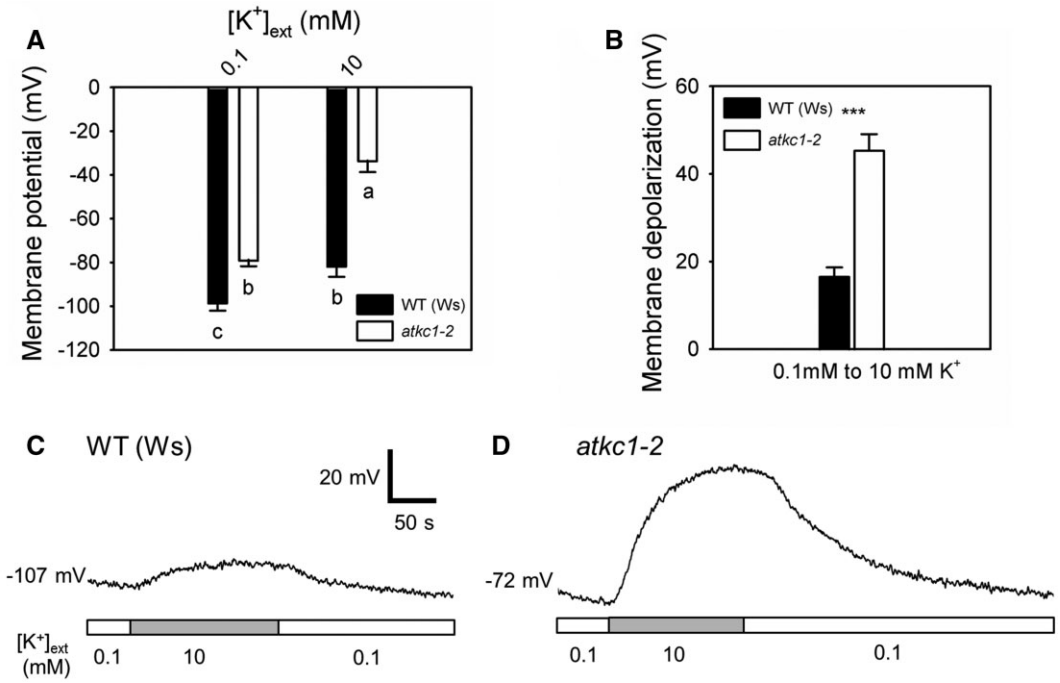

Figure 7 The *atkc1–2* mutation results in membrane depolarization in pavement cells and in an increased sensitivity of the MP to the external concentration of K^+. A, MPs recorded in WT and *atkc1–2* pavement cells bathed in 0.1 mM or 10 mM K^+. B, Membrane depolarizations induced by the increase in external K^+ concentration from 0.1 to 10 mM. Each value corresponded to the difference in the MP that was observed when the external K^+ concentration was increased from 0.1 mM to 10 mM K^+ within the same cell. C, Representative trace of a WT pavement cell showing membrane depolarization and repolarization due to changes in external K^+ concentration. D, Representative trace of an *atkc1–2* pavement cell subjected to the same protocol as in (C). White and gray bars depict the periods where the external K^+ concentration was 0.1 and 10 mM, respectively. In (A) and (B), means ± SE are shown. $n = 14$ cells from five different plants for WT and $n = 14$ cells from three different plants for *atkc1–2*. Letters depict significant group values after ANOVA and Tukey's post hoc test. *** denotes $P < 0.001$ in a two-tailed Student's *t* test.

ProGL2:AtKC1, *ProAt1G66460:AtKC1*, and *ProFMO1:AtKC1* (Figure 8A). The results in Supplemental Figure S1 indicate that *ProKCS19* and *ProOCT3* are active in both guard cells and pavement cells, and for the latter, in hydathodes as well. *ProGL2* and *ProAt1G66460* are active only in trichomes, and *ProFMO1* is active only in hydathodes (Supplemental Figure S1).

In contrast to the above, two constructs complemented the phenotype as efficiently as *ProAtKC1:AtKC1* (Figure 4B). These were *ProCER5:AtKC1* and *ProCYP96A4:AtKC1* (Figure 8A). The *GUS* staining data displayed in Supplemental Figure S1 indicate that *ProCER5* (shown to be epidermis-specific; Pighin et al., 2004) is active in guard cells, pavement cells, hydathodes, and trichomes (abaxial and adaxial sides). *ProCYP96A4* (also leaf epidermis-specific as shown by Mustroph et al., 2009) is active in guard cells, pavement cells, and trichomes (abaxial and adaxial sides) but not in hydathodes. It should be noted that leaves of Ws ecotype plants harbor trichomes at both the abaxial and adaxial faces (Telfer et al., 1997; Supplemental Figure S5) and that the *atkc1–2* mutation did not affect trichome density on either face (Supplemental Figure S6).

In a second series of experiments, both the *ProCER5:AtKC1* and *ProCYP96A4:AtKC1* constructs were found to also restore the stomatal aperture to the WT non-monotonic mode in responding to rising external mannitol concentration—in contrast to *ProKAT1:AtKC1* (Figure 8B compared with Figure 6C)—and the level of K^+ accumulation in leaf epidermis (Figure 8C compared with Figure 5).

By cross-comparing these data, complementation of the defect in stomatal aperture control of *atkc1–2* plants required *AtKC1* expression not only in surrounding pavement cells but, unexpectedly, also in trichomes. However, targeted transgenic expression in only trichomes by two different specific promoters (*ProGL2* and *ProAt1G66460*) did not rescue the *atkc1–2* phenotype.

Discussion

Relative to autonomous stomatal control, the non-autonomous regulatory mechanism is conceptually more abstract, as there had been a paucity of functionally defined genetic or molecular components. Neither had there been detailed knowledge on the precise cell types from which these components operated, nor their physiological modes of action. We report here that the inactivation of *AtKC1* results in larger stomatal apertures and increased transpirational water loss. *AtKC1* encodes a silent Shaker channel subunit because it does not form functional K^+ channels on its own (see below). The *atkc1–2* mutation was not compensated by transgenic expression of *AtKC1* only in guard cells within the leaf epidermis using the promoter of the Shaker channel gene *KAT1* (Figure 4B). The dominant-negative approach by

Table 1 Summary of the results presented in Supplemental Figure S1 (expression pattern) and Figure 8A (stomatal aperture)

AtKC1 expression in	Promoter								
	Pro AtKC1	*Pro CER5*	*Pro CYP96A4*	*Pro KCS19*	*Pro OCT3*	*Pro KAT1*	*Pro GL2*	*Pro At1G66460*	*Pro FMO1*
Guard cells	+	+	+	+	+	+	–	–	–
Pavement cells	+	+	+	+	+	–	–	–	–
Trichomes	+	+	+	–	–	–	+	+	–
Hydathodes	+	+	–	–	+	–	–	–	+
Stomatal aperture similar to that in WT plants	Yes	Yes	Yes	No	No	No	No	No	No

expressing *ProKAT1:AtKC1–DN* (Supplemental Figure S4) proved that *ProKAT1* remained active in the guard cells throughout our experiment. Altogether, these results suggested that *AtKC1* does not control stomatal aperture from within the guard cells, but that it contributes to the non-autonomous mechanism that opposes the guard cells' outward push.

Turgor pressures of the guard cell and surrounding pavement cells have rarely been directly measured. Due to their small size, Arabidopsis guard cells are not easily amenable to investigations using the classical pressure probe methodology (Franks et al., 1995, 1998, 2001). We have therefore used an atomic force microscope (Beauzamy et al., 2015) to assess the amount of hydrostatic pressure required to cause indentation on guard cells and pavement cells. This methodology, which is not destructive, basically applies a non-penetrative indentation with an elastic probe on the sample surface (Beauzamy et al., 2015). The applied force can be linearly deduced from the measured probe deformation, while the mechanical properties of the sample can be deduced from the applied force and sample surface deformation due to indentation. Turgor pressure is further deduced using established continuum mechanics equations of the inflated shell model (Beauzamy et al., 2015). This approach has been applied to epidermal cells in cotyledon (Verger et al., 2018), a system histologically similar to leaves, and in shoot apical meristem (Long et al., 2020). Following these two studies, we deduced turgor pressure using forces at depth ranges that minimize the influence of neighboring cells and of underlying cell layers or cavities (Malgat et al., 2016; Long et al., 2020).

The turgor pressure values deduced in the present study for WT Arabidopsis guard cells and pavement cells (close to 2 and 1 MPa, respectively, in open stomata; Figure 6A) are within the range of values previously obtained by pressure probe applied to *Vicia faba* and *Tradescantia virginiana*, which ranged from 1 to 5 MPa for guard cells, and from 0.6 to 1 MPa for pavement cells (Franks et al., 1995, 1998). In all of these studies, pavement cells exhibited lower turgor pressure than guard cells. In Arabidopsis, the difference in turgor between guard cells and pavement cells observed in our experimental conditions is close to 0.8 MPa, which indicates that the osmolyte content of pavement cells was significantly lower than that of guard cells, by about ~330 mOsm L^{-1}.

The AFM data did not reveal any significant difference in guard cell turgor between the WT and *atkc1–2*. In contrast, the turgor pressure of pavement cells was weaker in *atkc1–2* than in the WT, by about 0.15 MPa, that is by ca. 20% (Figure 6A). This decrease in turgor corresponds to a decrease in osmoticum concentration by about 60 mOsm L^{-1}. Such a difference is supported by the 40–60 mOsm L^{-1} difference in mannitol concentration required to induce epidermal cell plasmolysis in WT and *atkc1–2* plants as deduced from Figure 6B (the curves of the WT and *atkc1–2*-mutant plants being shifted from each other by about 40–60 mOsm L^{-1}). Such differences are also consistent with the observation that the internal concentration of K^+ in epidermal strips was about 42–58 mM lower in the mutant plants (as computed from Figures 5 and 8C, respectively, FW/DW ratio = 9). Thus, the decrease in pavement cell turgor revealed by microindentation in the *atkc1–2* mutant can be mainly ascribed to lower K^+ accumulation in these cells.

Because *AtKC1* is a member of the Shaker K^+ channel family, its absence may disturb the steady-state accumulation of K^+ in diverse tissue types. The *atkc1–2* mutation has been found to affect neither whole root, whole shoot nor whole leaf K^+ contents (Jeanguenin et al., 2011; Figure 5). Thus, the decrease in leaf epidermal strip K^+ contents resulting from this mutation appears to be limited to this tissue. The observation that the *ProCER5:AtKC1* and *ProCYP96A4:AtKC1* constructs complemented the mutant defect in epidermal strip K^+ content (Figure 8C) and in stomatal aperture control (Figure 8A and B) while the promoters *ProCER5* and *ProCYP96A4* are known to be essentially active in leaf epidermis (Pighin et al., 2004; Mustroph et al., 2009; Supplemental Figure S1) provides further evidence that both defects have their origin in the leaf epidermis and not in another plant tissue.

MP measurements indicated that the *atkc1–2* mutation resulted in a significant depolarization of pavement cells, by about 20 or 48 mV when the external solution contained 0.1 or 10 mM K^+, respectively (Figure 7A). The magnitude of the depolarization induced by the 100-fold increase in the external K^+ concentration was thus much larger in the mutant than in the WT pavement cells (Figure 7, B–D). Altogether, these results provide evidence that the absence of *AtKC1* functional expression impacted electrical features within the leaf epidermis. The decrease in membrane polarization resulting from the *atkc1–2* mutation is consistent with—and could result from or contribute to—the lower K^+ content of mutant pavement cells (Figures 5, 6, and 8C).

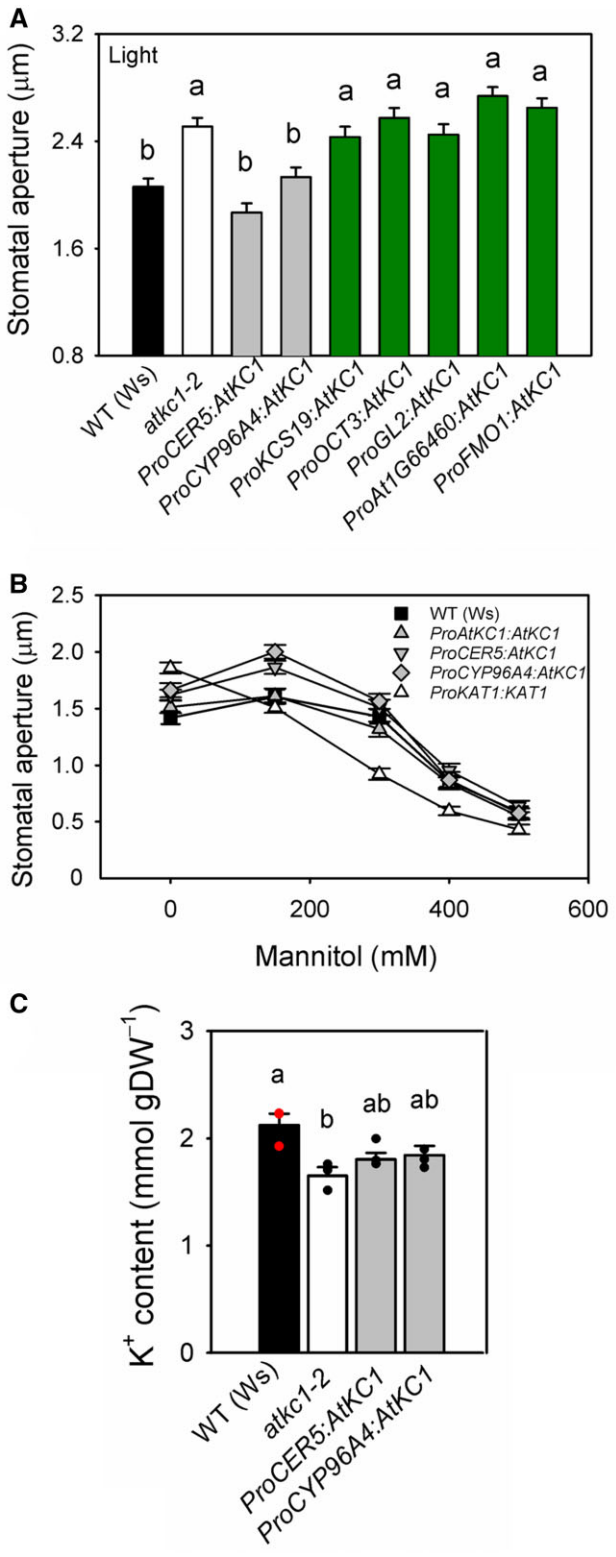

Figure 8 Restoration of WT stomatal features in the *atkc1–2* mutant requires *AtKC1* expression in pavement cells and trichomes. A, Stomatal aperture under light in WT Arabidopsis plants (Ws ecotype, black bar), in *atkc1–2*-mutant plants (white bar), and in *atkc1–2*-mutant plants transformed with a construct allowing expression of *AtKC1* under control of one of the following promoters: *ProCER5*, *ProCYP96A4*, *ProKCS19*, *ProOCT3*, *ProGL2*, *ProAt1G66460*, and *ProFMO1* (expression patterns of these promoters: see Table 1 and Supplemental Figures S1 and S5). Gray bars and dark green bars: transformed plants with rescued or non-rescued stomatal phenotype, respectively. Stomatal aperture was measured following the same procedure as in Figure 1D. B, Stomatal aperture in epidermal strips bathed in mannitol solutions. Transformed lines identified in (A) as displaying stomatal aperture values similar to that of WT plants (transforming constructs: *ProAtKC1:AtKC1*, *ProCER5:AtKC1*, and *ProCYP96A4:AtKC1*) also behaved like WT plants in response to added mannitol (showing a non-monotonous sensitivity to mannitol concentration). In contrast, the transgenic line *ProKAT1:AtKC1*, shown in (A) to display a stomatal aperture similar to that of *atkc1–2*-mutant plants, also displayed a monotonous decrease in stomatal aperture in response to increased mannitol concentration, and thus behaved like *atkc1–2*-mutant plants (see Figure 6C). C, Leaf epidermis K^+ content in WT plants, in *atkc1–2*-mutant plants and in *atkc1–2*-mutant plants transformed with the *ProCER5:AtKC1* and *ProCYP96A4:AtKC1* complementing constructs. A–C, Means ± SE. In (A) and (B), n = 94–131 stomata from six leaves. In (C), n = 3 pools of samples, each one obtained from nine leaves. In (A) and (C), letters depict significant group values after ANOVA and Tukey's post hoc test.

The increase in the sensitivity of the MP to K^+ external concentration, which indicates an increase in the membrane conductance to K^+ in the mutant, when compared with the WT, is consistent with the fact that *AtKC1* behaves as a negative regulator of inward Shaker channels (Jeanguenin et al., 2011). Indeed, *AtKC1* does not form homotetrameric channels on its own, as indicated above, but can form heteromeric channels upon interaction with co-expressed inwardly rectifying Shaker channel subunits, leading to increased diversity in channel functional properties (Reintanz et al., 2002; Duby et al., 2008; Geiger et al., 2009; Honsbein et al., 2009; Jeanguenin et al., 2011; Zhang et al., 2015; Wang et al., 2016). The activation potential of heteromeric channels associating *AtKC1* to *KAT1*, *KAT2*, or *AKT2* is shifted toward more negative values, when compared with *KAT1*, *KAT2*, or *AKT2* homomeric channels (Duby et al., 2008; Jeanguenin et al., 2011). Such a negative regulation has been proposed to prevent K^+ efflux (loss) when the MP is less negative than the K^+ equilibrium potential (E_K) but more negative than the (homomeric) channel-activation potential (Duby et al., 2008; Jeanguenin et al., 2011).

Patch-clamp analysis revealed different types of current patterns among protoplasts derived from pavement cells recognizable by their size and shape, and in particular the fact that they did not possess chloroplasts. Thus, this analysis provides evidence that, within the leaf epidermis, cells that are neither guard cells nor trichomes (the latter cells being not digested by the enzyme cocktail in our experimental conditions) do not form a homogeneous tissue in terms of plasma membrane electrical properties. Evidence is available at the molecular level that the generic term of "pavement cells" actually belies a functionally heterogeneous population of cells, based on the criterion of gene expression markers. For instance, *PATROL1* is expressed in guard cells and only in the smallest of the immediately adjacent

pavement cells. The other two surrounding pavement cells do not express this gene to detectable levels. PATROL1 directs trafficking of certain proteins, including AHA1/OST2, a proton pump that is important for hyperpolarization of the plasma membrane (Merlot et al., 2007; Higaki et al., 2014). Moreover, single-cell gene transcriptomic profiling in the epidermis of Arabidopsis has revealed differences between pavement cells and basal trichome cells (also named socket or skirt cells) (Lieckfeldt et al., 2008; Schliep et al., 2010; Zhou et al., 2017). This diversity in gene expression, as well as the diversity in membrane electrical properties revealed by our patch-clamp recordings, might be related to the positional information sensed by the epidermal cells with respect to veins, trichomes, and/or stomata.

None of the different types of current patterns displaying no time-dependent slowly activating component (Supplemental Figure S3) is reminiscent of the activity of a cloned and functionally characterized ion channel. The situation is different for the protoplasts displaying a Shaker-like time-dependent activation (Figure 3). Indeed, the available transcriptome data (EMBL-EBI expression atlas) as well as *GUS* reporter gene analysis (Lacombe et al., 2000) indicate that, together with *AtKC1*, the Shaker gene *AKT2* is expressed in pavement cells. Thus, the Shaker-like slowly activating weakly inwardly rectifying current pattern (Figure 3) that was observed in about one-third or one-quarter (in the WT and the mutant, respectively) of the pavement cell protoplasts suggests that a significant part of the inward and outward currents was mediated by *AKT2* homomeric and heteromeric channels comprising, in WT plants, *AtKC1* subunits since both *AKT2* and *AKT2-AtKC1* channels have been shown to be weakly rectifying (Jeanguenin et al., 2011). The weak rectification of *AKT2* results from coexistence in the membrane of two populations of channels, one displaying activation by increasingly negative voltages and the other displaying an instantaneously activated non-rectifying ("leak-like") behavior, depending on the channel phosphorylation status (Michard et al., 2005a, 2005b). Such phosphorylation-controlled variations of the channel gating properties could also contribute to the diversity of plasma membrane electrical behavior among pavement cell protoplasts.

Comparison of the patch-clamp recordings in WT and *atkc1–2* pavement cell protoplasts did not provide evidence that the pavement cell diversity in plasma membrane electrical features was reduced by the mutation (Figure 3 and Supplemental Figure S3). The *I–V* curves derived for the WT and *atkc1–2*-mutant protoplasts displaying a time-dependent slowly activating *AKT2*-like component are quite similar (Figure 3H). This suggests that it is not by affecting the time-dependent *AKT2*-like conductance that the *atkc1–2* mutation alters the pavement cell K^+ content (Figures 5, 6, and 8) and the sensitivity of pavement cell MP to K^+ (Figure 7).

Altogether, these patch-clamp data leave the actual impact of the mutation on the K^+ conductance of (the different types of) pavement cells still elusive. Patch-clamp measurements on protoplasts provide information about individual cell (protoplast) properties, while MP measurements give access to data reflecting in situ (in the leaf apoplastic solution) integrated (within the leaf epidermis as a whole due to electrical connection through plasmodesmata) electrical properties. Such a difference, together with the large diversity in K^+ conductance among pavement cells and the fact that the present patch-clamp analysis has essentially taken into account the protoplasts whose membrane inward conductance appeared to be dominated by a time-dependent slowly activating conductance (Figure 3), might explain that no significant difference between *atkc1–2* mutant and WT pavement cell protoplasts has been evidenced by this analysis.

It should also be noted that *AtKC1* is known to play a role in exocytosis, besides its contribution to the regulation of inwardly rectifying Shaker channel activity. It interacts with the SNARE *AtSYP121* (Honsbein et al., 2009), a vesicle-trafficking protein active at the plasma membrane and mediating vesicle fusion required for cellular homeostasis and growth (Geelen et al., 2002). Formation of tripartite complexes associating *AtSYP121* to *AtKC1*, itself associated to the other Shaker subunit of the heteromeric channel, has been shown to confer voltage sensitivity to the contribution of *AtSYP121* to vesicle fusion at the plasma membrane, rendering the secretion voltage dependent, a process proposed to couple K^+ uptake to exocytosis and to maintain turgor pressure in growing plant cells (Honsbein et al., 2009; Grefen et al., 2015). Finally, screening tests using a split ubiquitin derived system suggest that *AtKC1* might also interact with a ROP protein (Rho-of-Plant, a Rho GTPase) as well as a nitrate transporter (Obrdlik et al., 2004).

Fused to the *AtKC1* coding sequence, cell-type-specific promoters directing expression in guard cells, or in both guard cells and pavement cells, or in trichomes only, did not complement the *atkc1*-mutant stomatal phenotype, while complementation was observed with promoters directing expression in these three cell types together (Figure 8). Considering the whole set of observations, the simplest hypothesis is that *AtKC1* contributes to non-autonomous guard cell control of stomatal aperture and that this contribution involves pavement cells and trichomes.

A salient finding from the patch-clamp recordings in pavement cell protoplasts is that, despite the observed diversity in cell membrane electrical properties (Figure 3 and Supplemental Figure S3), pavement cells possess in common a rather weak level of rectification when compared with that displayed by guard cells (Figure 2). The model suggested by these results is thus that guard cells, with strong rectification of both inward and outward K^+ conductances, are embedded in a layer of cells mostly displaying weak rectification. It is tempting to assume that this functional differentiation between pavement cells and guard cells renders the exchanges of K^+ between these two types of cells immediately dependent on the guard cell membrane transport activity. The quasi-linearity of the *I–V* curve of pavement

cells would allow that any change in K^+ apoplastic concentration due to uptake of this cation by—or release from—guard cells could modulate the efflux of K^+ from—or influx into—pavement cells. In other words, due to their low level of rectification, pavement cells could be a permanent and immediately available K^+ source or sink, depending on the demand of guard cells, in agreement with the model that guard cells play the dominant motor role in stomatal movements. Finally, the low level of rectification of pavement cells, which allows K^+ exchanges in the whole range of MPs, can also be hypothesized to facilitate K^+ exchange/shuttling among the pavement cells themselves.

The mutant defect in stomatal movements observed in planta (Figure 1C) is not likely to directly result from altered control of K^+ availability in the external solution (i.e. in the leaf epidermis apoplast) since impaired control of stomatal aperture was also observed in vitro in epidermal strips bathed in a solution containing a high concentration of K^+ (Figures 1D, 4B, and 8A), like that used in microindentation experiments (Figure 6A). Our results suggest that, when AtKC1 is functional, trichomes cooperate with adjacent epidermal cells in K^+ homeostasis. *ProAtKC1*, as well as *ProCER5* and *ProCYP96A4*, which complemented the *atkc1–2* mutant, are all expressed in the ring of basal cells skirting the base of the trichome. The major class of transcripts detected in trichomes, basal, and epidermal cells belongs to transport and transport-associated proteins (Lieckfeldt et al., 2008), suggesting that these cells are particularly active in intra- and intercellular movements of solutes. Absence of *AtKC1* functional expression might affect K^+ distribution between trichomes, basal cells, and pavement cells, resulting in a reduction of K^+ accumulation in the latter cells.

In conclusion, the whole set of results supports the following causal chain: absence of *AtKC1* functional expression leads to a reduced steady-state K^+ accumulation in pavement cells and thereby in a decrease in the turgor of these cells. The weakened backpressure of the epidermal cells therefore surrenders to the opposing guard cell turgor, constitutively resulting in more open stomata. The present data provide genetic, molecular, and electrophysiological evidence that complex K^+ distribution among several epidermal cell types contributes to stomatal aperture outcome. In conclusion, these data support the view that the entire epidermis should be regarded as a dynamic filter controlling stomatal aperture.

Materials and methods

Plant culture

Arabidopsis thaliana (Ws) plants were grown in a growth chamber, at 20°C, with a 8-/16-h light/dark photoperiod (300 µmol photons m^{-2} s^{-1}, white light from fluorescent tubes), at 70% RH (RH = relative air humidity), in commercial compost. They were used for experiments when they were 6-weeks old and still not bolting.

Stomatal aperture and transpiration measurements

Rosette transpirational water loss, preparation of leaf epidermal strips, and measurements of stomatal aperture (in 30 mM KCl and 10 mM KOH-MES, pH 6.5) were performed as previously described (Hosy et al., 2003; Nieves-Cordones et al., 2012). Stomatal aperture measurements were performed in triplicate on at least six epidermal strips from six different plants. To study the effect of increased mannitol concentration on stomatal aperture, epidermal strips were incubated in stomatal opening buffer containing 30 mM KCl and 10 mM KOH-MES, pH 6.5, under light for 2 h and then transferred into dishes containing the same solution plus different concentrations of mannitol. Images were taken within 5 min incubation under a microscope (Olympus BH2) coupled to a color camera (Olympus Color View II). Displayed data are mean of at least 100 values per treatment and per mannitol concentration (when stated) for each plant genotype. All experiments were conducted in blind, that is genotypes unknown to the experimenter until data had been analyzed. Vital staining with neutral red at 0.02% (w/v) was performed to confirm the viability of guard cells and other epidermal cells in epidermal strips. For whole-plant transpiration assays, pots containing individually grown 6-week-old plants subjected to the same watering regime were sealed with a plastic film to prevent water loss from the substrate. The soil water content was initially adjusted to 2.5 g of H_2O per g of dry soil. Evapotranspirational water loss was then compensated by addition of equivalent amounts of water in order to maintain the water content at its initial value over a four-day period. Pots were weighed twice a day, at dusk and at dawn, for determination of transpirational water loss (in milliliters H_2O per square centimeter of leaf and per hour). Foliar area was measured with ImageJ from images of rosettes. Stomatal conductance was measured on intact leaves with a diffusion porometer (AP4; Delta-T Devices).

Patch-clamp recordings

WT and *atkc1–2* *A. thaliana* Ws plants were grown for 6 weeks in compost (individual containers) in a growth chamber (20°C, 65% relative humidity, 8-h/16-h light/dark, 250 µmol m^2 s^1). Electrophysiological analyses on guard cell protoplasts were performed as previously described (Hosy et al., 2003; Lebaudy et al., 2008). Epidermal cell protoplasts were isolated by enzymatic digestion of leaf epidermal strips in darkness. The digestion solution contained 1-mM $CaCl_2$, 2-mM ascorbic acid, 1-mM MES-KOH (pH 5.5), Onozuka RS cellulase (1% w/v, Duchefa Biochemie, Haarlem, Netherlands), and Y-23 pectolyase (0.1% w/v, Seishin Pharmaceutical, Tokyo, Japan). The osmolarity was adjusted to 500 mosM with D-mannitol. The epidermal strips were digested for 35 min at 27°C. Filtration through 50-µm mesh allowed recovery of protoplasts. The filtrate was rinsed four times with two volumes of conservation buffer: 100-mM potassium glutamate, 10-mM $CaCl_2$, 10-mM HEPES, the osmolarity being adjusted to 520 mOsm with D-mannitol, and the pH to 7.5 with KOH. The protoplast suspension was allowed

to sediment and then kept on ice in darkness in the conservation buffer, which was also used as external solution for the sealing step. Patch-clamp pipettes were pulled (P07, DMZ-Universal Puller, Zeitz-Instruments, Germany) from borosilicate capillaries (GC150TF-7.5, Phymep, France). The pipette solution contained 1-mM $CaCl_2$, 5-mM EGTA, 0.5-mM $MgCl_2$, 100-mM potassium glutamate, 2-mM Mg-ATP, and 20-mM HEPES. The osmolarity of the solution was adjusted to 540 mOsm with D-mannitol and the pH was adjusted to 7.5 with KOH (final K^+ concentration assayed by flame spectrophotometry: ca. 140 mM). Under these conditions, the pipette resistance was about 18 MΩ. Seals with resistance >1 GΩ were used for electrophysiological analyses. The bath solution contained, except when otherwise mentioned, 100-mM potassium glutamate, 0.1-mM $CaCl_2$, 10-mM HEPES, the osmolarity being adjusted to 520 mOsm with D-mannitol, and the pH to 7.5 with KOH (final K^+ concentration: 105 mM, assayed by flame spectrophotometry). Whole-cell recordings were obtained using an Axon Instruments Axopatch 200B amplifier. pCLAMP 8.2 software (Axon Instruments, Foster City, CA, USA) was used for voltage pulse stimulation, online data acquisition, and data analysis. The voltage protocol consisted of stepping the MP from −40 mV (holding potential) to +80 mV or −205 mV, or from +25 mV (holding potential) to either +130 mV or −140 mV, in 15 mV steps. Liquid junction potentials at the pipette/bath interface were measured and corrected.

MP recordings in pavement cells

Rosette leaves from WT and *atkc1–2*-mutant plants grown in hydroponics for 3 weeks (1/5 Hoagland solution) were excised and immobilized in a 1-mL chamber. The external solution contained 5-mM MES (2-(*N*-Morpholino) ethanesulfonic acid), 0.1-mM KCl, 0.1-mM $CaCl_2$, and 0.1-mM NaCl, brought to pH 6.0 with $Ca(OH)_2$. The leaf was bathed for at least 30 min in the perfusion solution before cell impalement. Impalement microelectrodes were pulled from borosilicate glass capillaries (1B120F-4, World precision instruments, http://www.wpiinc.com) and showed a diameter of approximately 0.5 µm at the tip. Glass microelectrodes were fixed to electrode holders containing an Ag/AgCl pellet and connected to a high-impedance amplifier (model duo 773; World precision instruments). Impalement and reference electrodes were filled with 200-mM KCl. To impale leaf pavement cells, the microelectrode was approached to the leaf surface with a motorized micromanipulator (Narishige MM-89, http://narishige-group.com) and impalements were carried out with a one-axis oil hydraulic micromanipulator (Narishige MO-10). The precise penetration of the microelectrode into pavement cells was visually followed with an inverted microscope.

Atomic force microscopy

AFM determination of turgor pressure in the leaf epidermis was performed as in Beauzamy et al. (2015) with modifications. Specifically, 1 × 1 cm leaf segments were fixed in Petri-dishes by double-sided tape and microtube tough-tags (Diversified Biotech) with the abaxial face up. Adaxial trichomes were removed by tweezers to facilitate tape fixation. Leaf segments were incubated in the stomata opening buffer (see above) under light for at least 2 h before being mounted onto a BioScope Catalyst AFM (Bruker). A spherical-tipped AFM cantilever with 400 nm tip radius and 42 N/m spring constant was used for the measurements (SD-SPHERE-NCH-S-10, Nanosensors); a spherical tip was used to avoid the cell wall puncture that often occurs upon usage of a more standard sharp pyramidal tip. One to 2-µm-deep indentations were made along the topological skeletons of epidermal cells to ensure relative normal contact between the probe and sample surface. At least three indentation positions were chosen for each cell, with each position consecutively indented three times, making at least nine indentation force curves per cell. Cell recordings of AFM force curves were performed with the NanoIndentation plugin for ImageJ (https://fiji.sc/) as described in Long et al. (2020). Parameters for turgor deduction were generated as follows. The cell wall elastic modulus and apparent stiffness were calculated from each force curve following Beauzamy et al. (2015). To minimize the effect of neighboring and underlying cells (Malgat et al., 2016; Long et al., 2020), we used a force range of 1%–10% of maximal force for modulus and 75%–99% of maximal force for cell stiffness, which typically correspond to depths in the ranges 10–100 and 400–500 nm, respectively. Cell surface curvature was estimated from AFM topographic images, with the curvature radii fitted to the long and short axes of small cells or along and perpendicular to the most prominent topological skeleton of heavily serrated pavement cells. Turgor pressure was further deduced from each force curve (four iterations) with the simplified hypothesis that the surface periclinal cell walls of leaf epidermis have a constant thickness, at 200 nm, and cell-specific turgor pressure is retrieved by averaging all turgor deductions per cell.

Plasmolysis assays

Epidermal strips were peeled, fixed on glass slides, and bathed in solutions differing in mannitol concentration. The percentage of strips displaying plasmolysis within 5 min incubation was determined using a microscope.

Tissue K^+ content

Leaf margins were isolated by obtaining 2-mm razor-cut bands, which were enriched for hydathodes. Leaf epidermis was obtained by peeling abaxial epidermis with forceps. K^+ contents were determined in dried samples by flame spectrometry (SpectrAA 220 FS, Varian, http://www.varianinc.com/), after ionic extraction (sample incubation for 2 days in 0.1 N HCl).

Complementation of *atkc1–2*-mutant plants and promoter analyses

Mutant isolation and generation of transgenic plants expressing *AtKC1* under its native promoter has been described elsewhere (Jeanguenin et al., 2011). For guard cell-

specific complementation of *atkc1–2*-mutant plants, *AtKC1* and *AtKC1–DN* cDNAs were expressed under the *KAT1* promoter in pCambia1301 vector (Hajdukiewicz et al., 1994). *AtKC1-DN* has been described previously (Jeanguenin et al., 2011) and contained two pore residue mutations (G291R and Y292R) that rendered it a dominant-negative channel subunit. For other indicated cell-specific expression of *AtKC1*, we cloned the previously characterized genomic regions upstream of the first ATG from the loci *CER5*, *OCT3*, *GL2*, *At1G66460*, and *FMO1* in the pCambia1301 vector to drive *AtKC1* expression. For expression pattern analyses, the same upstream regions were also cloned in pGWB3 using Gateway cloning (Nakagawa et al., 2007) to drive *GUS* expression in WT transformed plants, except *ProOCT3:GUS* lines that were kindly gifted by Isabell Kufner and described elsewhere (Kufner and Koch, 2008). For previously uncharacterized promoters (*ProCYP96A4* and *ProKCS19*), the inter-genomic regions located between the first ATG and the 3′-end of the corresponding upstream loci were amplified. Floral dip method was used to transfect Arabidopsis plants (Clough and Bent, 1998). Transformed lines were verified by RT-PCR on RNA extracted from leaves of individual T1 plants, and T2 progeny homozygous for the transgene were selected based on true segregation of the linked hygromycin resistance marker of pCambia1301. Experiments were conducted on T3 homozygous plants.

Guard cell protoplast preparation for gene expression analysis

About 30–35 fully expanded rosette leaves were kept in cold water and in the dark. Main veins of leaves were removed using a scalpel. Leaf pieces were blended three times for 45 s at full speed, and the yielded mixture was put over a nylon mesh and rinsed with cold distilled water. The epidermis fragments recovered from the 75-µm nylon mesh were digested for 30–45 min at 25°C with gentle shaking (140 rpm) in an enzyme solution (0.7% Calbiochem cellulysin, 0.1% PVP 40, 0.25% BSA, 0.5 mM ascorbic acid, 45% distilled water, and 55% solution containing sorbitol 560 mmol/kg, 5 mM MES, 0.5 mM $CaCl_2$, 0.5 mM $MgCl_2$, 0.5 mM ascorbic acid, pH 5.5 with Tris). Translation inhibitor (100 mg/L Cordycepin, C3394-Sigma) and transcription inhibitor (33 mg/L Actinomycin D, A1410- Sigma) were also added to the digestion mixture. The digestion process was followed under a microscope (Olympus BH2), to check that "intact" guard cells were still present in situ in the digested epidermis at the end of the enzymatic treatment. The undigested fraction was recovered by filtration through 40-µm nylon mesh, rinsed with basic solution, and stored at −80°C.

Gene expression analysis by RT-qPCR

Total RNA extraction, synthesis of first-strand cDNAs, and quantitative RT–PCR procedures were performed as described elsewhere (Cuellar et al., 2010). Primers used for real time qRT-PCR were designed using PRIMER3 (http://frodo.wi.mit.edu) (Supplemental Table S2). All amplification plots were analyzed with an Rn threshold (normalized reporter) of 0.2 to obtain C_T (threshold cycle) values. Standard curves for *AtKC1*, *KAT1*, *KAT2*, and *GORK* were obtained from dilution series of known quantities of corresponding cDNA fragments used as templates. Standard curves were used to calculate the absolute numbers of tested cDNA molecules in each cDNA sample and these values were then normalized against corresponding housekeeping gene signals. Four housekeeping genes *EF1alpha*, *TIP41*, *PDF2*, and *MXC9.20* (Czechowski et al., 2005) were used to calculate a normalization factor with the online algorithm "geNorm" (https://genorm.cmgg.be/).

Expression analyses by *GUS* staining

GUS staining of leaves from 6-week-old transgenic plants expressing the β-*GUS* reporter gene under the control of the promoters listed in Supplemental Figure S1 was performed as described elsewhere (Lagarde et al., 1996). Similar expression patterns were obtained in three independent transgenic lines for each promoter.

Statistical analysis

Statistical analysis was performed using the two-tailed Student's *t* test, analysis of variance (ANOVA), and Tukey's post hoc test as indicated with Statistix V.8 software for Windows. The results are shown in Supplemental Data Set S1.

Accession numbers

Sequence data from this article can be found in the TAIR (Arabidopsis) database under accession numbers: *AtKC1* (At4G32650), *KAT1* (AT5G46240), *CER5* (At1G51500), *OCT3* (At1G16390), *GL2* (At1G79840), *Uncharacterized Protein Kinase* gene (At1G66460), *FMO1* (At1G19250), *CYP96A4* (At5G52320), and *ProKCS19* (At5G04530).

Supplemental data

The following materials are available in the online version of this article.

Supplemental Figure S1. Expression patterns driven by the *AtKC1* promoter and other selected cell-specific promoters in leaf epidermis.

Supplemental Figure S2. Stomatal density in WT and *atkc1–2* leaves (abaxial side).

Supplemental Figure S3. Example of non-Shaker-like channel activities in pavement cell protoplasts from *A. thaliana* WT and *atkc1–2*-mutant plants (Ws ecotype).

Supplemental Figure S4. Expression of *AtKC1* and *AtKC1–DN* under the *KAT1* promoter.

Supplemental Figure S5. Expression patterns driven by *AtKC1* promoter and other selected cell-specific promoters in abaxial leaf epidermis and trichomes.

Supplemental Figure S6. The *atkc1–2* mutation does not affect trichome density in WT and *atkc1–2* plants.

Supplemental Table S1. Cell-specific expression level of the genes selected in complementation experiments (Figure 8) obtained from eFP browser site (supports Figure 8).

Supplemental Table S2. Primer list.
Supplemental Data Set S1. Statistical analysis results.

Acknowledgments

We thank Isabell Kufner for providing *ProOCT3:GUS* lines.

Funding

This work was supported by the Alfonso Martin Escudero Foundation (to M.N.-C.), the Marie Curie Programme (Grant No. 272390 FP7-IEF to M.N.-C.), and the European Research Council (PhyMorph #307387 to A.B.).

Conflict of interest statement. None declared.

References

Bauer H, Ache P, Lautner S, Fromm J, Hartung W, Al-Rasheid KA, Sonnewald S, Sonnewald U, Kneitz S, Lachmann N, et al. (2013) The stomatal response to reduced relative humidity requires guard cell-autonomous ABA synthesis. Curr Biol **23**: 53–57

Beauzamy L, Derr J, Boudaoud A (2015) Quantifying hydrostatic pressure in plant cells by using indentation with an atomic force microscope. Biophys J **108**: 2448–2456

Blatt MR (2000) Cellular signaling and volume control in stomatal movements in plants. Annu Rev Cell Dev Biol **16**: 221–241

Britto DT, Coskun D, Kronzucker HJ (2021) Potassium physiology from Archean to Holocene: A higher-plant perspective. J Plant Physiol **262**: 153432

Clough SJ, Bent AF (1998) Floral dip: A simplified method for Agrobacterium-mediated transformation of *Arabidopsis thaliana*. Plant J **16**: 735–743.

Cuellar T, Pascaud F, Verdeil JL, Torregrosa L, Adam-Blondon AF, Thibaud JB, Sentenac H, Gaillard I (2010) A grapevine Shaker inward K^+ channel activated by the calcineurin B-like calcium sensor 1-protein kinase CIPK23 network is expressed in grape berries under drought stress conditions. Plant J **61**: 58–69

Czechowski T, Stitt M, Altmann T, Udvardi MK, Scheible WR (2005) Genome-wide identification and testing of superior reference genes for transcript normalization in Arabidopsis. Plant Physiol **139**: 5–17

Daram P, Urbach S, Gaymard F, Sentenac H, Chérel I (1997) Tetramerization of the AKT1 plant potassium channel involves its C-terminal cytoplasmic domain. EMBO J **16**: 3455–3463

Duby G, Hosy E, Fizames C, Alcon C, Costa A, Sentenac H, Thibaud JB (2008) AtKC1, a conditionally targeted Shaker-type subunit, regulates the activity of plant K^+ channels. Plant J **53**: 115–123

Franks PJ, Cowan IR, Farquhar GD (1998) A study of stomatal mechanics using the cell pressure probe. Plant Cell Environ **21**: 94–100

Franks PJ, Buckley TN, Shope JC, Mott KA (2001) Guard cell volume and pressure measured concurrently by confocal microscopy and the cell pressure probe. Plant Physiol **125**: 1577–1584

Franks PJ, Cowan IR, Tyerman SD, Cleary AL, Lloyd J, Farquhar GD (1995) Guard-cell pressure aperture characteristics measured with the pressure probe. Plant Cell Environ **18**: 795–800

Geelen D, Leyman B, Batoko H, Di Sansebastiano GP, Moore I, Blatt MR (2002) The abscisic acid-related SNARE homolog NtSyr1 contributes to secretion and growth: Evidence from competition with its cytosolic domain. Plant Cell **14**: 387–406

Geiger D, Becker D, Vosloh D, Gambale F, Palme K, Rehers M, Anschuetz U, Dreyer I, Kudla J, Hedrich R (2009) Heteromeric AtKC1·AKT1 channels in Arabidopsis roots facilitate growth under K^+-limiting conditions. J Biol Chem **284**: 21288–21295

Gray A, Liu L, Facette M (2020) Flanking support: How subsidiary cells contribute to stomatal form and function. Front Plant Sci **11**: 1–12

Grefen C, Karnik R, Larson E, Lefoulon C, Wang Y, Waghmare S, Zhang B, Hills A, Blatt MR (2015) A vesicle-trafficking protein commandeers Kv channel voltage sensors for voltage-dependent secretion. Nat Plants **1**: 15108

Hajdukiewicz P, Svab Z, Maliga P (1994) The small, versatile pPZP family of Agrobacterium binary vectors for plant transformation. Plant Mol Biol **25**: 989–994

Hedrich R (2012) Ion channels in plants. Physiol Rev **92**: 1777–1811

Higaki T, Hashimoto-Sugimoto M, Akita K, Iba K, Hasezawa S (2014) Dynamics and environmental responses of PATROL1 in Arabidopsis subsidiary cells. Plant Cell Physiol **55**: 773–780

Honsbein A, Sokolovski S, Grefen C, Campanoni P, Pratelli R, Paneque M, Chen Z, Johansson I, Blatt MR (2009) A tripartite SNARE-K^+ channel complex mediates in channel-dependent K^+ nutrition in Arabidopsis. Plant Cell **21**: 2859–2877

Hosy E, Vavasseur A, Mouline K, Dreyer I, Gaymard F, Porée F, Boucherez J, Lebaudy A, Bouchez D, Véry A-A, et al. (2003) The Arabidopsis outward K^+ channel GORK is involved in regulation of stomatal movements and plant transpiration. Proc Natl Acad Sci USA **100**: 5549–5554

Humble GD, Raschke K (1971) Stomatal opening quantitatively related to potassium transport: Evidence from electron probe analysis. Plant Physiol **48**: 447–453

Jakoby MJ, Falkenhan D, Mader MT, Brininstool G, Wischnitzki E, Platz N, Hudson A, Hulskamp M, Larkin J, Schnittger A (2008) Transcriptional profiling of mature Arabidopsis trichomes reveals that NOECK encodes the MIXTA-like transcriptional regulator MYB106. Plant Physiol **148**: 1583–1602

Jammes F, Leonhardt N, Tran D, Bousserouel H, Véry A-A, Renou J-P, Vavasseur A, Kwak JM, Sentenac H, Bouteau F, et al.. (2014) Acetylated 1,3-diaminopropane antagonizes abscisic acid-mediated stomatal closing in Arabidopsis. Plant J **79**: 322–333

Jeanguenin L, Alcon C, Duby G, Boeglin M, Chérel I, Gaillard I, Zimmermann S, Sentenac H, Véry A-A (2011) AtKC1 is a general modulator of Arabidopsis inward Shaker channel activity. Plant J **67**: 570–582

Jegla T, Busey G, Assmann SM (2018) Evolution and structural characteristics of plant voltage-gated K^+ Channels. Plant Cell **30**: 2898–2909

Jezek M, Blatt MR (2017) The membrane transport system of the guard cell and its integration for stomatal dynamics. Plant Physiol **174**: 487–519

Jezek M, Hills A, Blatt MR, Lew VL (2019) A constraint-relaxation-recovery mechanism for stomatal dynamics. Plant Cell Environ **42**: 2399–2410

Jin X, Wang RS, Zhu M, Jeon BW, Albert R, Chen S, Assmann SM (2013) Abscisic acid-responsive guard cell metabolomes of Arabidopsis wild-type and *gpa1* G-protein mutants. Plant Cell **25**: 4789–4811

Kim TH, Bohmer M, Hu H, Nishimura N, Schroeder JI (2010) Guard cell signal transduction network: Advances in understanding abscisic acid, CO_2, and Ca^{2+} signaling. Annu Rev Plant Biol **61**: 561–591

Kufner I, Koch W (2008) Stress regulated members of the plant organic cation transporter family are localized to the vacuolar membrane. BMC Res Notes **1**: 43

Lacombe B, Pilot G, Michard E, Gaymard F, Sentenac H, Thibaud JB (2000) A shaker-like K^+ channel with weak rectification is expressed in both source and sink phloem tissues of Arabidopsis. Plant Cell **12**: 837–851

Lagarde D, Basset M, Lepetit M, Conejero G, Gaymard F, Astruc S, Grignon C (1996) Tissue-specific expression of Arabidopsis AKT1 gene is consistent with a role in K^+ nutrition. Plant J **9**: 195–203

Lebaudy A, Vavasseur A, Hosy E, Dreyer I, Leonhardt N, Thibaud JB, Véry A-A, Simonneau T, Sentenac H (2008) Plant adaptation to fluctuating environment and biomass production are strongly dependent on guard cell potassium channels. Proc Natl Acad Sci USA **105**: 5271–5276

Lebaudy A, Pascaud F, Véry A-A, Alcon C, Dreyer I, Thibaud J-B, Lacombe B (2010) Preferential KAT1-KAT2 heteromerization determines inward K^+ current properties in Arabidopsis guard cells. J Biol Chem **285**: 6265–6274

Leonhardt N, Kwak JM, Robert N, Waner D, Leonhardt G, Schroeder JI (2004) Microarray expression analyses of Arabidopsis guard cells and isolation of a recessive abscisic acid hypersensitive protein phosphatase 2C mutant. Plant Cell **16**: 596–615

Lieckfeldt E, Simon-Rosin U, Kose F, Zoeller D, Schliep M, Fisahn J (2008) Gene expression profiling of single epidermal, basal and trichome cells of *Arabidopsis thaliana*. J Plant Physiol **165**: 1530–1544

Long Y, Cheddadi I, Mosca G, Mirabet V, Dumond M, Kiss A, Traas J, Godin C, Boudaoud A (2020) Cellular heterogeneity in pressure and growth emerges from tissue topology and geometry. Curr Biol **30**: 1504–1516.e8

MacRobbie EAC (1980) Osmotic measurements on stomatal cells of *Commelina communis* L. J Membr Biol **53**: 189–198

Malgat R, Faure F, Boudaoud A (2016) A mechanical model to interpret cell-scale indentation experiments on plant tissues in terms of cell wall elasticity and turgor pressure. Front Plant Sci **7**: 1351

Merlot S, Leonhardt N, Fenzi F, Valon C, Costa M, Piette L, Vavasseur A, Genty B, Boivin K, Muller A, et al. (2007) Constitutive activation of a plasma membrane H^+-ATPase prevents abscisic acid-mediated stomatal closure. EMBO J **26**: 3216–3226

Michard E, Dreyer I, Lacombe B, Sentenac H, Thibaud JB (2005a) Inward rectification of the AKT2 channel abolished by voltage-dependent phosphorylation. Plant J **44**: 783–797

Michard E, Lacombe B, Porée F, Mueller-Roeber B, Sentenac H, Thibaud JB, Dreyer I (2005b) A unique voltage sensor sensitizes the potassium channel AKT2 to phosphoregulation. J Gen Physiol **126**: 605–617

Misra BB, Acharya BR, Granot D, Assmann SM, Chen S (2015) The guard cell metabolome: Functions in stomatal movement and global food security. Front Plant Sci **6**: 334

Mott KA, Buckley TN (2000) Patchy stomatal conductance: Emergent collective behaviour of stomata. Trends Plant Sci **5**: 258–262

Mustroph A, Zanetti ME, Jang CJ, Holtan HE, Repetti PP, Galbraith DW, Girke T, Bailey-Serres J (2009) Profiling translatomes of discrete cell populations resolves altered cellular priorities during hypoxia in Arabidopsis. Proc Natl Acad Sci USA **106**: 18843–18848

Nakagawa T, Kurose T, Hino T, Tanaka K, Kawamukai M, Niwa Y, Toyooka K, Matsuoka K, Jinbo T, Kimura T (2007) Development of series of gateway binary vectors, pGWBs, for realizing efficient construction of fusion genes for plant transformation. J Biosci Bioeng **104**: 34–41

Nakamura RL, McKendree WL Jr, Hirsch RE, Sedbrook JC, Gaber RF, Sussman MR (1995) Expression of an Arabidopsis potassium channel gene in guard cells. Plant Physiol **109**: 371–374

Nguyen TH, Huang S, Meynard D, Chaine C, Michel R, Roelfsema MRG, Guiderdoni E, Sentenac H, Véry A-A (2017) A dual role for the OsK5.2 ion channel in stomatal movements and K^+ loading into Xylem Sap. Plant Physiol **174**: 2409–2418

Nieves-Cordones M, Caballero F, Martinez V, Rubio F (2012) Disruption of the *Arabidopsis thaliana* inward-rectifier K^+ channel AKT1 improves plant responses to water stress. Plant Cell Physiol **53**: 423–432

Nieves-Cordones M, Chavanieu A, Jeanguenin L, Alcon C, Szponarski W, Estaran S, Chérel I, Zimmermann S, Sentenac H, Gaillard I (2014) Distinct amino acids in the C-linker domain of the Arabidopsis K^+ channel KAT2 determine its subcellular localization and activity at the plasma membrane. Plant Physiol **164**: 1415–1429

Olszak B, Malinovsky FG, Brodersen P, Grell M, Giese H, Petersen M, Mundy J (2006) A putative flavin-containing mono-oxygenase as a marker for certain defense and cell death pathways. Plant Sci **170**: 614–623

Obrdlik P, El-Bakkoury M, Hamacher T, Cappellaro C, Vilarino C, Fleischer C, Ellerbrok H, Kamuzinzi R, Ledent V, Blaudez D, et al. (2004) K^+ channel interactions detected by a genetic system optimized for systematic studies of membrane protein interactions. Proc Natl Acad Sci USA **101**: 12242–12247

Palevitz BA, Hepler PK (1985) Changes in dye coupling of stomatal cells of Allium and Commelina demonstrated by microinjection of Lucifer yellow. Planta **164**: 473–479

Pandey S, Zhang W, Assmann SM (2007) Roles of ion channels and transporters in guard cell signal transduction. FEBS Lett **581**: 2325–2336

Pighin JA, Zheng H, Balakshin LJ, Goodman IP, Western TL, Jetter R, Kunst L, Samuels AL (2004) Plant cuticular lipid export requires an ABC transporter. Science **306**: 702–704

Pilot G, Gaymard F, Mouline K, Chérel I, Sentenac H (2003) Regulated expression of Arabidopsis shaker K^+ channel genes involved in K^+ uptake and distribution in the plant. Plant Mol Biol **51**: 773–787

Pilot G, Lacombe B, Gaymard F, Chérel I, Boucherez J, Thibaud JB, Sentenac H (2001) Guard cell inward K^+ channel activity in Arabidopsis involves expression of the twin channel subunits KAT1 and KAT2. J Biol Chem **276**: 3215–3221

Reintanz B, Szyroki A, Ivashikina N, Ache P, Godde M, Becker D, Palme K, Hedrich R (2002) AtKC1, a silent Arabidopsis potassium channel alpha-subunit modulates root hair K^+ influx. Proc Natl Acad Sci USA **99**: 4079–4084

Roelfsema MRG, Prins HBA (1997) Ion channels in guard cells of *Arabidopsis thaliana* (L.) Heynh. Planta **202**: 18–27

Rohaim A, Gong LD, Li J, Rui H, Blachowicz L, Roux B (2020) Open and closed structures of a barium-blocked potassium channel. J Mol Biol **432**: 4783–4798

Schliep M, Ebert B, Simon-Rosin U, Zoeller D, Fisahn J (2010) Quantitative expression analysis of selected transcription factors in pavement, basal and trichome cells of mature leaves from Arabidopsis thaliana. Protoplasma **241**: 29–36

Schroeder JI, Raschke K, Neher E (1987) Voltage dependence of K^+ channels in guard-cell protoplasts. Proc Natl Acad Sci USA **84**: 4108–4112

Spalding EP, Hirsch RE, Lewis DR, Qi Z, Sussman MR, Bryan DL (1999) Potassium uptake supporting plant growth in the absence of AKT1 channel activity. J Gen Physiol **113**: 909–918

Su YH, North H, Grignon C, Thibaud JB, Sentenac H, Véry AA (2005) Regulation by external K^+ in a maize inward shaker channel targets transport activity in the high concentration range. Plant Cell **17**: 1532–1548

Szymanski DB, Jilk RA, Pollock SM, Marks MD (1998) Control of GL2 expression in Arabidopsis leaves and trichomes. Development **125**: 1161–1171

Talbott LD, Zeiger E (1996) Central roles for potassium and sucrose in guard-cell osmoregulation. Plant Physiol **111**: 1051–1057

Telfer A, Bollman KM, Poethig RS (1997) Phase change and the regulation of trichome distribution in *Arabidopsis thaliana*. Development **124**: 645–654

Tominaga M, Kinoshita T, Shimazaki K-I (2001) Guard-cell chloroplasts provide ATP required for H^+ pumping in the plasma membrane and stomatal opening. Plant Cell Physiol **42**: 795–802

Urbach S, Chérel I, Sentenac H, Gaymard F (2000) Biochemical characterization of the Arabidopsis K^+ channels KAT1 and AKT1 expressed or co-expressed in insect cells. Plant J **23**: 527–538

Verger S, Long Y, Boudaoud A, Hamant O (2018) A tension-adhesion feedback loop in plant epidermis. Elife **7**: 1–25

Véry A-A, Sentenac H (2002) Cation channels in the Arabidopsis plasma membrane. Trends Plant Sci **7**: 168–175

Véry A-A, Sentenac H (2003) Molecular mechanisms and regulation of K^+ transport in higher plants. Annu Rev Plant Biol **54**: 575–603

Véry A-A, Nieves-Cordones M, Daly M, Khan I, Fizames C, Sentenac H (2014) Molecular biology of K^+ transport across the plant cell membrane: What do we learn from comparison between plant species? J Plant Physiol **171**: 748–769

Wang RS, Pandey S, Li S, Gookin TE, Zhao Z, Albert R, Assmann SM (2011) Common and unique elements of the ABA-regulated transcriptome of Arabidopsis guard cells. BMC Genomics **12**: 216

Wang XP, Chen LM, Liu WX, Shen LK, Wang FL, Zhou Y, Zhang Z, Wu WH, Wang Y (2016) AtKC1 and CIPK23 synergistically modulate AKT1-mediated low-potassium stress responses in Arabidopsis. Plant Physiol **170**: 2264–2277

Wegner LH, De Boer AH, Raschke K (1994) Properties of the K^+ inward rectifier in the plasma membrane of xylem parenchyma cells from barley roots: Effects of TEA^+, Ca^{2+}, Ba^{2+} and La^{3+}. J Membr Biol **142**: 363–379

Wille AC, Lucas WJ (1984) Ultrastructural and histochemical studies on guard cells. Planta **160**: 129–142

Zhang B, Karnik R, Wang Y, Wallmeroth N, Blatt MR, Grefen C (2015) The Arabidopsis R-SNARE VAMP721 interacts with KAT1 and KC1 K^+ channels to moderate K^+ current at the plasma membrane. Plant Cell **27**: 1697–1717

Zhao Z, Zhang W, Stanley BA, Assmann SM (2008) Functional proteomics of *Arabidopsis thaliana* guard cells uncovers new stomatal signaling pathways. Plant Cell **20**: 3210–3226

Zhou LH, Liu SB, Wang PF, Lu TJ, Xu F, Genin GM, Pickard BG (2017) The Arabidopsis trichome is an active mechanosensory switch. Plant Cell Environ **40**: 611–621

Zhu M, Assmann SM (2017) Metabolic signatures in response to abscisic acid (ABA) treatment in *Brassica napus* Guard cells revealed by metabolomics. Sci Rep **7**: 12875